Published OnlineFirst October 18, 2011; DOI:10.1158/0008-5472.CAN-11-0034

Molecular and Cellular Pathobiology

Cancer Research

HB-EGF and PDGF Mediate Reciprocal Interactions of Carcinoma Cells with Cancer-Associated Fibroblasts to Support Progression of Uterine Cervical Cancers

Takuya Murata[1,3], Hiroto Mizushima[2], Ichino Chinen[2], Hiroki Moribe[2], Shigeo Yagi[4], Robert M. Hoffman[5,6], Tadashi Kimura[3], Kiyoshi Yoshino[3], Yutaka Ueda[3], Takayuki Enomoto[3], and Eisuke Mekada[2]

Abstract

Tumor stroma drives the growth and progression of cancers. A heparin-binding epidermal growth factor–like growth factor, HB-EGF, is an EGF receptor ligand that stimulates cell growth in an autocrine or paracrine fashion. While elevated expression of HB-EGF in cancer cells and its contribution to tumor progression are well documented, the effects of HB-EGF expression in the tumor stroma have not been clarified. Here, we show that HB-EGF is expressed in stromal fibroblasts where it promotes cancer cell proliferation. In uterine cervical cancers, HB-EGF was detected immunohistochemically in the stroma proximal to the cancer epithelium. Proliferation of cervical cancer cells *in vitro* was enhanced by coculture with fibroblasts isolated from tumor tissues of patients with cervical cancer. Inhibition of HB-EGF function or treatment with platelet-derived growth factor (PDGF) inhibitors abrogated cancer cell growth enhanced by cervical cancer–associated fibroblast (CCF) coculture. Furthermore, tumor formation in a mouse xenograft model was enhanced by cotransplantation of CCF or mouse embryonic fibroblasts, but not with embryonic fibroblasts from HB-EGF–deficient mice. Conversely, conditioned medium from cancer cells induced HB-EGF expression in CCF. Mechanistic investigations established that PDGF was the primary factor responsible. Together, our findings indicate that HB-EGF and PDGF reciprocally mediate the interaction of cancer cells with cancer-associated fibroblasts, promoting cancer cell proliferation in a paracrine manner that has implications for novel combinatorial cancer therapies. *Cancer Res; 71(21); 6633–42. ©2011 AACR.*

Introduction

Tumor-surrounding tissues or the tumor stroma influence the behavior of carcinomas (1). The tumor stroma consists of extracellular matrix (ECM) and various types of cells including fibroblasts, immune and inflammatory cells, and blood vessel cells. Invasive carcinoma is often associated with expansion of the tumor stroma and increased deposition of ECM. Cancer cells can alter their adjacent stroma to form a permissive and supportive environment for tumor progression by producing growth factors, proteases, protease inhibitors, and ECM molecules. Fibroblasts within the tumor stroma, referred to as "cancer-associated fibroblasts" (CAF), have a modified phenotype and a prominent role in the progression, growth, and spread of cancers (2–4). Crosstalk between cancer cells and the stromal fibroblasts is assumed. Cancer cells secrete various kinds of growth factors that stimulate their own proliferation in an autocrine manner. Some cancer cell–secreted growth factors, including TGFβ, platelet-derived growth factor (PDGF), and fibroblast growth factor (FGF)-2, act as key mediators of fibroblast activation (2, 3, 5). The activated CAFs have a variety of effects on both cancer cells and the surrounding stroma. Their effects include altering the ECM environment, inducing an inflammatory response, and activating angiogenesis, as well as stimulating cancer cell proliferation and invasion by growth factor secretion. Thus, cancer–CAF interaction constitutes critical routes for cancer development and progression.

Cervical cancer is one of the most life-threatening diseases for women worldwide (6). Infection with human papilloma viruses (HPV) may be the first step of its carcinogenesis (7). Despite infection with HPV, most of the resultant precancerous lesions, termed squamous intraepithelial lesions (SIL), do not progress to an invasive carcinoma, suggesting that HPV does not act alone in the development of cervical cancer. Cervical cancer has a prominent stromal compartment. In the course of its progression, carcinoma cells invade the stroma, interact with fibroblasts, and change the stromal environment

Authors' Affiliations: [1]Obstetrics and Gynecology, Osaka-Saiseikai-Nakatsu Hospital; [2]Department of Cell Biology, Research Institute for Microbial Diseases, Osaka University; [3]Department of Obstetrics and Gynecology, Osaka University Graduate School of Medicine, Suita; [4]AntiCancer Japan Incorporated, Ibaraki, Osaka, Japan; [5]Department of Surgery, University of California San Diego; and [6]AntiCancer Inc., San Diego, California

Note: Supplementary data for this article are available at Cancer Research Online (http://cancerres.aacrjournals.org/).

Corresponding Author: Eisuke Mekada, Department of Cell Biology, Research Institute for Microbial Diseases, Osaka University, 3-1, Yamadaoka, Suita, Osaka 565-0871, Japan. Phone: 81-6-6879-8286; Fax: 81-6-6879-8289; E-mail: emekada@biken.osaka-u.ac.jp

doi: 10.1158/0008-5472.CAN-11-0034

Published OnlineFirst October 18, 2011; DOI:10.1158/0008-5472.CAN-11-0034

in a manner termed desmoplastic change or stromal reaction. Accordingly, the gene expression patterns of stromal cells are largely altered in cervical carcinogenesis (8). A study using a genetically-engineered mouse model suggested the presence of crosstalk between cancer cells and stromal fibroblasts, in which PDGF secreted from cancer cells stimulated PDGF receptor–expressing CAFs, leading to the induction of FGF-2 and FGF-7 production by CAFs which in turn stimulated angiogenesis and cancer cell proliferation (5).

Heparin-binding epidermal growth factor–like growth factor (HB-EGF) is an EGF receptor (EGFR) ligands, synthesized as a transmembrane precursor protein (pro-HB-EGF; ref. 9). Its extracellular domain is then cleaved by proteases, via the so-called ectodomain-shedding mechanism, which yields the soluble mature growth factor (sHB-EGF; ref. 10). sHB-EGF shows strong mitogenic and motility activity by acting through the EGFR (11–13). HB-EGF is involved in malignancy. Upregulation of HB-EGF has been reported in many types of malignant tumors (14–22). In the case of ovarian cancer, HB-EGF expression was increased in advanced cancers compared with that in normal ovaries and was associated with poor clinical outcome (14, 23). Although increasing evidence has accumulated on the role of HB-EGF in tumor cell growth and tumor progression (24), no study on the role of HB-EGF expressed in stromal fibroblasts has been reported.

Here, we show that HB-EGF is produced by stromal fibroblasts in uterine cervical cancer. Coculturing the human cervical cancer cell line ME180 with cervical cancer–associated fibroblasts (CCF) *in vivo* and *in vitro* indicated that stromal HB-EGF contributes to the enhanced proliferation of ME180 cells. On the other hand, PDGF produced in ME180 cells induced HB-EGF expression in fibroblasts, suggesting that these growth factors contribute to the reciprocal interaction of cancer cells and stromal fibroblasts.

Materials and Methods

Antibodies and reagents

Details about the antibodies and reagents are described in the Supplementary Materials and Methods.

Pathology scoring

HB-EGF immunostaining was simultaneously evaluated by 3 independent observers (including one gynecologic oncologist and one gynecologic pathologist), and a consensus was reached for each score. The positive reaction for HB-EGF was scored into 4 grades according to the following intensities of staining; 0, 1+, 2+, and 3+. The percentage of the positive staining area was also scored into the following 4 categories: 1 (0%–25%), 2 (26%–50%), 3 (51%–75%), and 4 (76%–100%). The sum of the intensity and percentage scores was used as the final staining score (25). The staining pattern of the frozen sections was defined as follows: 1, negative; 2–3, weak; 4–5, moderate; and 6–7, strong.

Cell culture

The cervical cancer cell line HeLa and squamous cell carcinoma (SCC)-derived ME180 cells were purchased from the American Type Culture Collection. The TCS and CaSki cell lines were obtained from the RIKEN BioResource Center. All the cell lines were passaged in our laboratory soon after receipt from cell banks, divided, and stocked in liquid nitrogen vessels. Each experiment was carried out using thawed cells without further authentication. Mouse embryonic fibroblast (MEF) cells from wild-type mice (MEF-HB$^{+/+}$) or HB-EGF knockout (KO) mice (MEF-HB$^{-/-}$) were obtained as described (26). All cell lines were maintained in Dulbecco's Modified Eagle's Medium (DMEM) supplemented with 10% FBS, 100 U/mL penicillin G, and 100 μg/mL streptomycin. CCF cells were obtained as described in the Supplementary Materials and Methods and cultured in DMEM supplemented with 20% FBS and antibiotics.

Coculture of ME180 cells and fibroblasts in 3-dimensional collagen gels

Unless otherwise stated, coculture assays were conducted under the following conditions. CCF cells (1×10^5) or MEF cells (1×10^5) were plated into 24-well plates 3 days before coculture experiments and cultured in 0.75 mL of DMEM containing 1% FBS. ME180 cells (2×10^2) were inoculated in 0.25 mL of 3-dimensional collagen gel (13) using a Falcon cell culture insert (0.4-μm pore size membrane; Becton Dickinson Labware). HB-EGF–neutralizing IgG (10 μg/mL), control goat IgG (10 μg/mL), CRM197 (500 ng/mL), or other inhibitors were added to the collagen gel. The cell culture inserts containing 3-dimensional–cultured ME180 cells were set into 24-well dishes at day 0 and cocultured for 14 days. The medium was changed on day 7 and a neutralizing antibody or control antibody was added to a final concentration of 10 μg/mL. On day 14, ME180 cells were recovered by treatment with collagenase and the viable cell numbers were counted (13). The effects of inhibitors on the growth of cervical cancer cells in coculture with CCF cells were expressed as a percentage of the control calculated by the following formula: total cell number of cervical cancer cells cocultured with CCF1 cells in the presence of a particular inhibitor divided by that of cervical cancer cells cocultured with CCF1 cells in the absence of a particular inhibitor × 100.

Mouse xenografting experiments

ME180 cells alone or mixtures of ME180 cells with either CCF cells or MEF cells were subcutaneously injected into the left flank of female athymic nude mouse at the cell numbers indicated in the figure legends. Unless otherwise stated, the tumor size was measured in 3 dimensions with calipers, and the tumor volume (mm^3) was calculated using the formula: $V = 0.52 \times \text{length} \times \text{width} \times \text{height}$.

Statistical analysis

Data are expressed as the mean ± SD. Statistical analysis of HB-EGF staining in various stages of cervical cancer progression was conducted with the χ^2 test. The statistical significance of other experimental data was evaluated using one-way ANOVA. Values of $P < 0.05$ were considered significant.

Published OnlineFirst October 18, 2011; DOI:10.1158/0008-5472.CAN-11-0034

Results

HB-EGF expression in the stroma of uterine cervical cancers and its correlation with cancer progression

Frozen sections of clinical samples were immunostained with an anti-human HB-EGF monoclonal antibody. In normal cervical tissues, the stroma was not immunostained, whereas the basal and parabasal epithelial layers were slightly reactive [Fig. 1A (i and ii)]. In cases with low-grade SILs (LSIL) and high-grade SILs (HSIL), faint immunostaining was observed in the stroma [Fig. 1A (iii–vi))] However, in cervical cancer tissues, HB-EGF was strongly immunostained in the stromal region [Fig. 1A (vii–xii)]. An irrelevant antibody did not immunostain the stroma, whereas a similar immunostaining pattern was observed with other anti-HB-EGF monoclonal antibodies (ref. 27; data not shown).

To evaluate the relationships between stromal HB-EGF immunostaining and clinical features, the cases with positive staining in the stroma and epithelium were scored (Fig. 1B, Supplementary Tables S1 and S2). No HB-EGF immunostaining was recorded in normal cervical stroma, whereas moderate to strong stromal HB-EGF immunostaining was observed in 33% of LSIL cases, 66% of HSIL cases, and all cases of SCC. In contrast, all the tissues had negative to weak immunostaining in the epithelium. These results indicate that HB-EGF protein is increased in the stromal tissues during cervical carcinogenesis, suggesting that it is involved in its progression. In addition, stromal HB-EGF immunostaining was observed in adenocarcinoma tissue and small cell carcinoma tissue, as well as in SCC of the uterine cervix (Supplementary Table S1 and Fig. S1).

Strong HB-EGF immunostaining was observed in stromal fibroblasts localized at the invasion front of cancerous epithelium [Fig. 1A (x and xii)]. The antibody used recognizes both pro-HB-EGF and sHB-EGF. HB-EGF has strong affinities for heparin-like molecules and heparan sulfate proteoglycans.

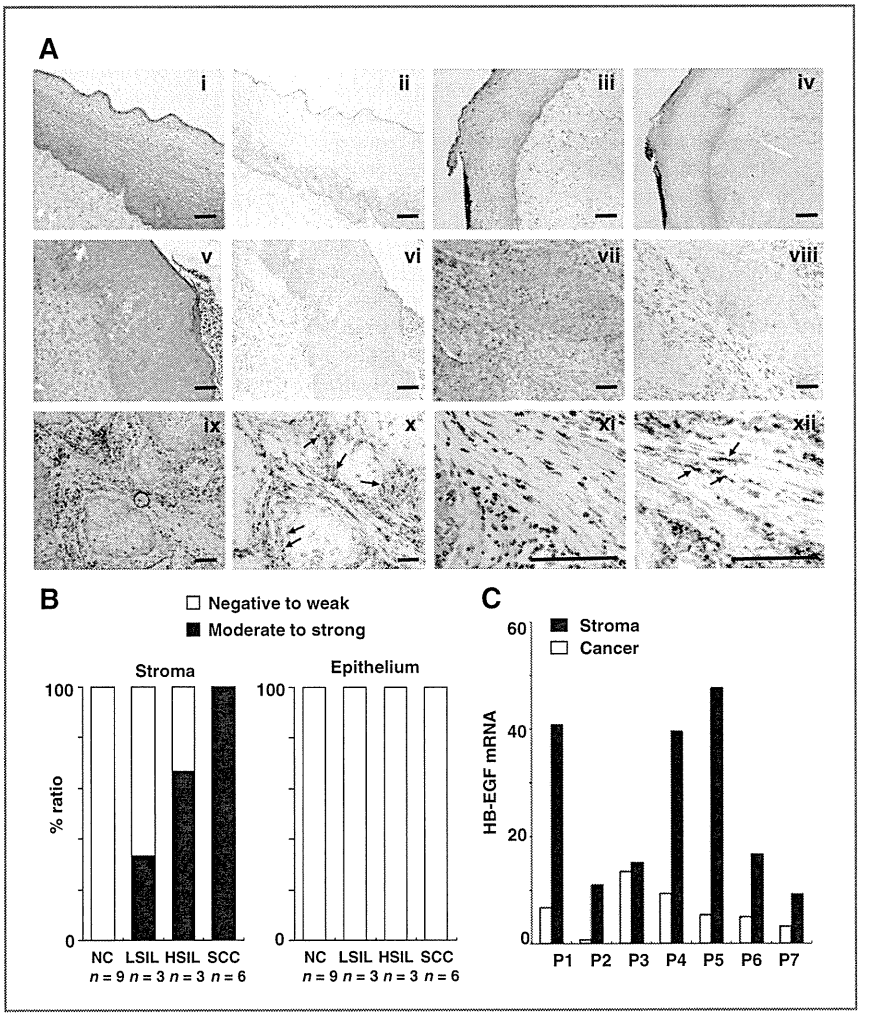

Figure 1. Expression of HB-EGF in cervical cancer stromata. A, hematoxylin and eosin (H&E) staining (i, iii, v, vii, ix, and xi) and immunohistochemical staining (brown; ii, iv, vi, vii, x, and xii) of normal cervix (i and ii), LSIL (iii and iv), HSIL (v and vi), and invasive SCC (vii–xii). Frozen sections of clinical samples were immunostained with an anti-human HB-EGF monoclonal antibody. Stromal cells contacting the invasion front of cancerous epithelial cells were strongly stained (x, arrows). HB-EGF was expressed in cancer-associated fibroblasts (xii, arrows). Bars, 0.1 mm. B, scoring of HB-EGF staining. A significant difference in the stromal staining of HB-EGF was observed between normal cervix (NC), LSILs, HSILs, and SCCs ($P = 0.011$; χ^2 test). C, laser microdissection revealed that HB-EGF was mainly expressed in stromal cells. P1 to P5 were tissues from patients with SCCs, whereas P6 and P7 were from patients with adenocarcinoma [$P = 0.009$ for P1–P7 ($n = 7$); $P = 0.015$ for P1–P5 ($n = 5$); one-way ANOVA].

Published OnlineFirst October 18, 2011; DOI:10.1158/0008-5472.CAN-11-0034

Thus, sHB-EGF might be deposited at the ECM-enriched stromal region, even though HB-EGF is not synthesized in stromal cells. To clarify which cells produce HB-EGF, cervical cancer cells, or cancer-surrounding stroma cells, the transcription levels of HB-EGF in cancer epithelium and stromal regions were determined by quantitative reverse transcription PCR using microdissected frozen tissues as described in the Supplementary Materials and Methods. For these assays, tissues from SCCs and adenocarcinoma of the uterine cervix were examined. As shown in Fig. 1C, HB-EGF mRNA was higher in the stroma than in the epithelium in total cervical cancer tissues ($n = 7$, $P = 0.009$) and in SCCs ($n = 5$, $P = 0.015$), indicating that HB-EGF is mainly produced by stroma cells of cervical cancer lesions.

HB-EGF produced by fibroblasts contributes to ME180 cell proliferation in a coculture system

The effect of stromal HB-EGF on cervical cancer cell proliferation was examined by coculture of ME180 cells with CCF1 cells derived from cervical cancer–associated fibroblasts (Fig. 2A). Because growth promotion by HB-EGF is masked in common monolayer culture (13), ME180 cells were embedded in collagen gel using cell culture inserts. These inserts have 0.4-μm diameter pores in the membrane, so that soluble factors can pass between the 2 chambers. The proliferation of ME180 cells was largely enhanced by coculture with CCF1 cells compared with ME180 cells cultured alone. ME180 cells, cocultured with CCF1 cells, formed larger cell colonies than ME180 cells without CCF1 cells (Fig. 2B). The total cell number of ME180 cells produced when cocultured with CCF1 cells was about 5 times greater than that of ME180 cells cultured alone (Fig. 2C). The enhanced cell growth by coculture with CCF1 cells was almost abrogated by an anti-HB-EGF neutralizing antibody, whereas growth inhibition by an anti-HB-EGF antibody was not observed in ME180 cells cultured alone (Fig. 2C). CRM197, which inhibits the mitogenic activity of HB-EGF (28), inhibited the cell growth of ME180 cells in the coculture system, but did not affect the growth of ME180 cells cultured alone (Fig. 2D). An EGFR inhibitor, erlotinib, also strongly inhibited the cell growth of ME180 cells in the coculture system but did not significantly affect the growth of ME180 cells cultured alone (Fig. 2E).

Enhanced proliferation by coculture with CCF1 cells was similarly observed in another cervical cancer cell line, CaSki cells, and the enhancement was inhibited by CRM197 (Supplementary Fig. S2). Enhanced proliferation of ME180 cells was also observed in coculture with MEF cells. ME180 cells were cocultured with either MEF cells derived from a wild-type mouse (MEF-HB$^{+/+}$) or MEF cells derived from an HB-EGF KO mouse (MEF-HB$^{-/-}$). The total cell number of ME180 cells produced when cocultured with MEF-HB$^{+/+}$ cells was about 8.5 times higher than that of ME180 cells cocultured with MEF-HB$^{-/-}$ cells (Fig. 2F). Thus, ME180 cell proliferation was enhanced by coculture with CCF or MEF cells, and HB-EGF produced by fibroblasts contributed to this enhancement.

The coculture experiments suggested that HB-EGF promotes ME180 cell proliferation by acting directly on ME180 cells through phosphorylation of their EGFR. However, it is

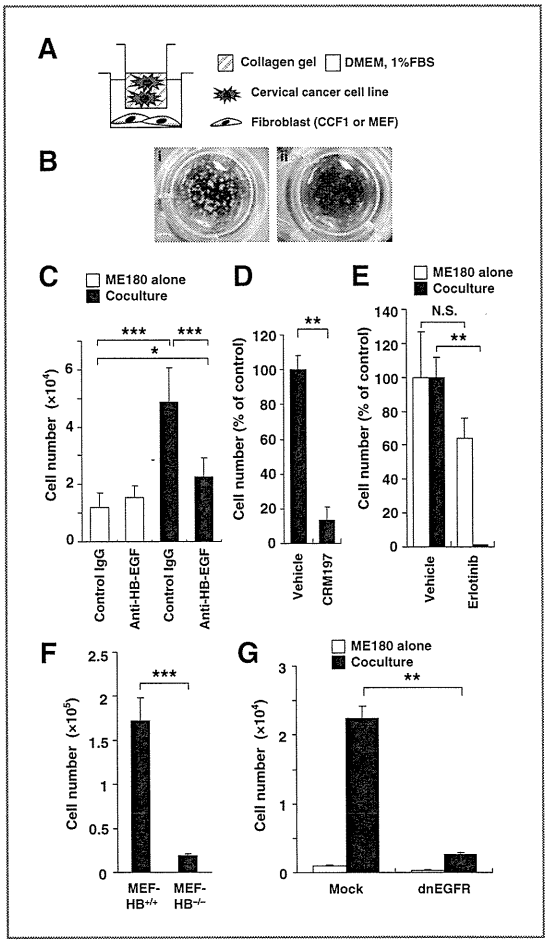

Figure 2. HB-EGF derived from fibroblasts enhances ME180 cell growth in coculture assays. A, scheme of the coculture system. B, ME180 cells were cocultured with (i) or without (ii) CCF1 cells for 14 days. C, an anti-HB-EGF antibody blocked the enhanced growth of ME180 cells cocultured with CCF1 cells. D and E, the HB-EGF inhibitor CRM197 (D) and EGFR inhibitor erlotinib (5 μmol/L; E) blocked the enhanced growth of ME180 cells cocultured with CCF1 cells. The total cell number is presented as the percentage of the control. F, ME180 cells were cocultured with MEF-HB$^{+/+}$ or MEF-HB$^{-/-}$ cells for 14 days. G, ME180 cells (2×10^3) infected with a control virus (mock) or a dnEGFR-expressing virus were cultured with or without CCF1 cells for 1 week. The bars indicate the mean ± SD of triplicate samples. *, $P < 0.05$; **, $P < 0.01$; and ***, $P < 0.005$.

also possible that HB-EGF acts on fibroblasts and indirectly enhances ME180 cell proliferation. To address this point, we carried out the following sets of experiments: First, addition of HB-EGF to the medium was found to enhance ME180 cell proliferation in the absence of CCF1 cells (Supplementary Fig. S3). Second, examination of EGFR expression and its phosphorylation revealed that ME180 cells expressed abundant EGFR and that its phosphorylation level was enhanced by coculture with CCF1 cells (Supplementary Fig. S4). Third, expression of dominant-negative (dn) EGFR in ME180 cells

Published OnlineFirst October 18, 2011; DOI:10.1158/0008-5472.CAN-11-0034

completely diminished the enhanced cell growth by coculture with CCF1 cells (Fig. 2G). These results indicate that HB-EGF directly enhances ME180 cell proliferation in coculture conditions through activation of EGFR on ME180 cells. HB-EGF binds to ErbB4, as well as to EGFR. However, ME180 cells had very low expression of ErbB4 (Supplementary Fig. S4). dnEGFR expression in ME180 cells completely inhibited the enhanced proliferation by coculture with CCF1 cells. Thus, ErbB4 is unlikely to contribute to this process.

Cotransplantation of fibroblasts enhances tumor growth in ME180 cells

To assess the contribution of fibroblasts and HB-EGF expressed in fibroblasts on tumor growth *in vivo*, we carried out cotransplantation experiments of ME180 cells with CCF or MEF cells into athymic nude mice. In the initial set of experiments, ME180 cells were used alone or mixed with various CCF cells (CCF1, CCF2, and CCF3) isolated from the cervical cancer stromata of different patients. Compared with ME180 cells alone, coinjection of ME180 cells with CCF1, CCF2, or CCF3 cells produced significantly larger tumors (Fig. 3A). The histology of the tumors showed a prominent stromal compartment, resembling SCC tissues of uterine cervical cancer (Fig. 3B). Immunostaining with an anti-human HB-EGF antibody showed the presence of human HB-EGF in fibroblasts surrounding the ME180 cells (Fig. 3B). Thus, the CCF cells enhanced the growth of ME180 cells in a mouse xenograft model to form tumors that were histologically similar to human uterine cervical cancer.

The enhanced tumor growth of ME180 cells by CCF cells was also examined by monitoring the tumor size using fluorescence imaging. Green fluorescent protein (GFP)-labeled ME180 (ME180/GFP) cells were subcutaneously transplanted with or without CCF1 cells into nude mice. Consistent with the results shown in Fig. 3A, fluorescence imaging confirmed that ME180 cell proliferation in the mouse xenograft model was enhanced by cotransplantation of CCF cells (Fig. 3C and D).

To examine whether stromal HB-EGF contributed to the enhanced tumor growth of the cervical cancer cells, ME180/GFP cells were mixed with either Ds-Red–labeled MEF-HB$^{-/-}$ (MEF-HB$^{-/-}$/Red) or Ds-Red–labeled MEF-HB$^{+/+}$ (MEF-HB$^{+/+}$/Red) cells and the mixtures were transplanted subcutaneously into nude mice. As shown in Fig. 3E and F, the tumors formed by ME180/GFP cells cotransplanted with MEF-HB$^{+/+}$/Red cells were approximately twice as large as those formed by ME180/GFP cells cotransplanted with MEF-HB$^{-/-}$/Red cells after 21 days. The latter tumors were similar in size to ME180 cells transplanted alone (see Fig. 3A and E), indicating that MEF-HB$^{-/-}$/Red cells did not enhance ME180 cell tumor growth. These results suggest that HB-EGF expressed in fibroblasts played a major role in accelerating the growth of ME180 cells in this mouse xenograft model.

Both hematoxylin and eosin and immunofluorescence staining (Fig. 3F) indicated that Ds-Red–positive MEF cells (red) were incorporated into the ME180/GFP tumors (green) in both the MEF-HB$^{+/+}$/Red and MEF-HB$^{-/-}$/Red transplantation experiments. Necrotic fields were more prevalent inside the tumor tissue when MEF-HB$^{-/-}$/Red cells were cotransplanted, compared with MEF-HB$^{+/+}$/Red cells, suggesting enhanced angiogenesis due to HB-EGF. Interestingly, the fluorescence intensity of ME180/GFP cells cotransplanted with MEF-HB$^{+/+}$/Red cells tended to be higher than that of ME180/GFP cells cotransplanted with MEF-HB$^{-/-}$/Red cells. GFP synthesis in the former combination might have resulted from a more abundant supply of nutrients and oxygen, given the enhanced angiogenesis in these tumors.

PDGF secreted by cervical cancer cells induces HB-EGF expression in fibroblasts

HB-EGF staining was preferentially observed at the stromal regions contacting the cancer invasion front. This suggested that cervical cancer cells might provide certain factors to the cancer-surrounding fibroblasts to induce the expression of HB-EGF and that fibroblasts could respond to these factors and upregulate HB-EGF mRNA synthesis. To test this hypothesis, conditioned media (CM) prepared from cervical cancer cell lines were added to the fibroblast primary cultures. When CM from CaSki or ME180 cells was added to CCF1 cells, the HB-EGF mRNA levels in CCF1 cells were markedly upregulated (Fig. 4A). Moderate upregulation was observed with CM from HeLa cells, whereas no upregulation was observed with CM from TCS or NIH3T3 cells (Fig. 4A). Enhanced HB-EGF mRNA expression by ME180 CM was observed in CCF2 and CCF3 cells as well as in CCF1 cells but not in ME180 cells themselves (Fig. 4B). Upregulation of HB-EGF mRNA expression was observed 3 hours after the addition of CM and peaked at 6 to 9 hours (Fig. 4C). Western blot analysis of CCF1 cell lysates confirmed the induction of HB-EGF protein synthesis by ME180 CM but not by control CM from CCF1 cells (Fig. 4D).

Examination of the expression levels of other EGFR ligands revealed that ME180 CM preferentially induced HB-EGF expression in CCF1 cells, although HeLa CM slightly induced epiregulin expression in these cells (Supplementary Fig. S5). These results indicate that CM from cervical cancer cell lines specifically induced HB-EGF among the EGFR family of growth factors in CCF cells.

To characterize the putative HB-EGF inducer in CM from ME180 cells, various inhibitors were tested to see whether they could prevent the induction of HB-EGF expression in CCF1 cells. FGF, insulin-like growth factor, PDGF, and TGFβ are known to be secreted by carcinoma cells to activate CAF cells. An FGF/VEGF receptor tyrosine kinase inhibitor, PD173074, did not inhibit HB-EGF expression in CCF1 cells, whereas the insulin-like growth factor receptor inhibitor AGL2263 and TGFβ RI kinase inhibitor II partially inhibited HB-EGF mRNA synthesis. In contrast, the PDGF receptor inhibitor AG1295 completely inhibited HB-EGF expression (Fig. 5A), suggesting that PDGF contributed to the HB-EGF induction in CCF cells. PDGF is composed of heterodimers or homodimers of 4 subtypes. To test whether PDGF could induce HB-EGF expression in CCF1 cells, various forms of PDGF were added to CCF1 cell cultures. PDGF-AB, PDGF-BB, and PDGF-DD induced HB-EGF expression in CCF1 cells, whereas PDGF-AA and PDGF-CC almost had no effect (Fig. 5B). Western blot analysis confirmed

Published OnlineFirst October 18, 2011; DOI:10.1158/0008-5472.CAN-11-0034

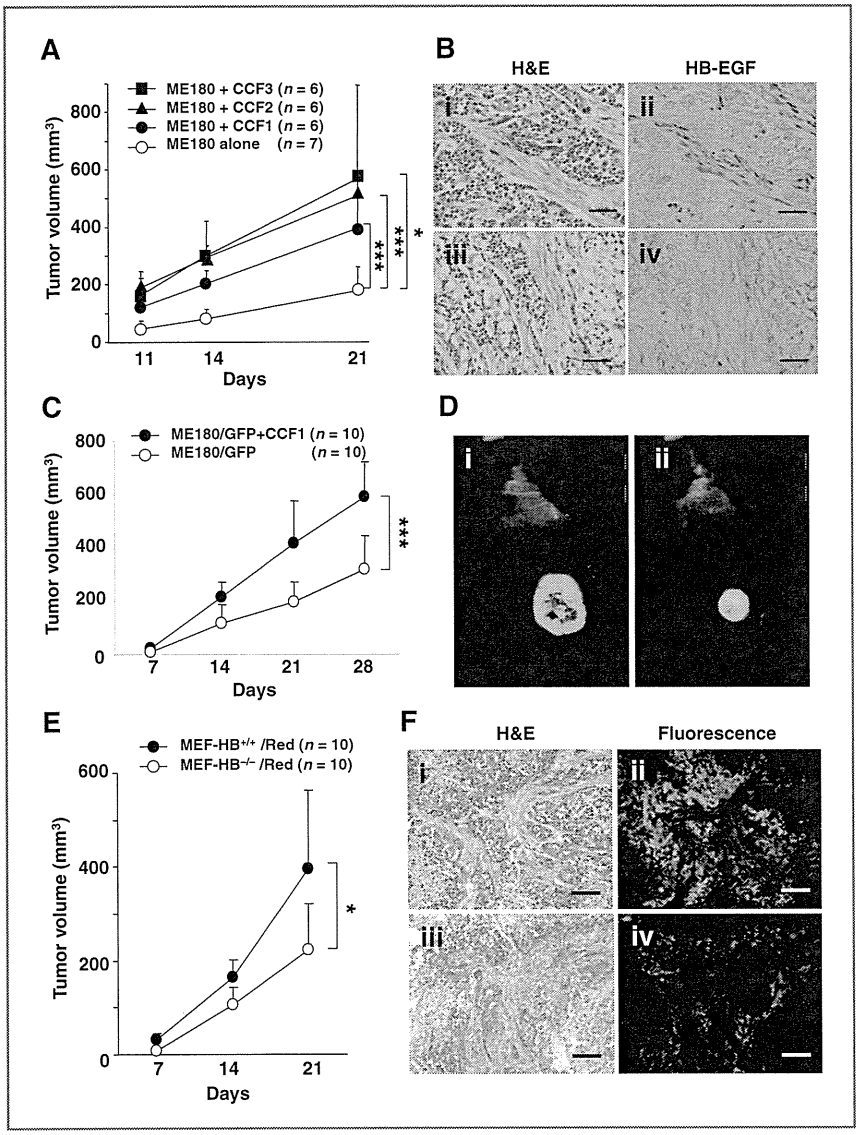

Figure 3. Coinjection of CCF or MEF cells with ME180 cells into athymic nude mice enhances ME180 tumor formation. A, ME180 cells alone (1.5×10^6) or ME180 cells (1.5×10^6) plus CCF cells (0.6×10^6) were injected subcutaneously, and the tumor volumes were measured. B, hematoxylin and eosin (H&E) staining (i and iii) and immunohistochemistry for HB-EGF (ii and iv) of tumor tissues generated by ME180 cells plus CCF1 cells (i and ii) or ME180 cells alone (iii and iv) in A. Bars, 50 μm. C, ME180/GFP cells alone (0.5×10^6) or ME180/GFP cells (0.5×10^6) plus CCF1 cells (2.5×10^6) were injected subcutaneously into nude mice, and the tumor volumes were measured by GFP fluorescence imaging. D, tumors formed by injection of ME180 cells alone (ii) or ME180 cells plus CCF1 cells (i) were observed by fluorescence imaging. E, ME180/GFP cells (1.0×10^6) were subcutaneously coinjected with MEF-HB$^{+/+}$/Red cells (5×10^6) or MEF-HB$^{-/-}$/Red cells (5×10^6) into nude mice. F, H&E-stained and fluorescence images of tumors formed by coinjection of ME180/GFP cells with MEF-HB$^{+/+}$/Red (i and ii) or MEF-HB$^{-/-}$/Red (iii and iv) cells. Cell nuclei were stained with Hoechst 33342 (blue). *, $P < 0.05$; ***, $P < 0.005$.

that ME180 cells produced PDGF-BB (Fig. 5C). Consistent with this result, CCF1 cells produced PDGFRβ (Supplementary Fig. S4). Moreover, tissue sections stained with anti-PDGF-B and anti-PDGFRβ antibodies indicated that these proteins were localized in cancer cells and the cancer-surrounding stromal region, respectively, in a mouse xenograft model coinjected with ME180 and CCF1 cells (Fig. 5D).

The PDGF receptor inhibitors AG1295 (Fig. 6A) and imatinib (Fig. 6B) prevented the enhanced proliferation of ME180 cells by coculture with CCF1 cells but did not inhibit ME180 cell proliferation when the cells were cultured alone (Fig. 6A and B). Coculture of CCF1 cells with ME180 cells resulted in PDGFRβ degradation in CCF1 cells (Supplementary Fig. S6), suggesting that the PDGFRβ activation by the ligand produced by ME180 cells was followed by ubiquitin-dependent degradation (29). Furthermore, the expression of dnPDGFRβ, but not that of dnEGFR, in CCF1 cells or MEF cells reduced the enhanced proliferation of ME180 cells by coculture with CCF1 or MEF cells (Fig. 6C). These results indicate that PDGF-BB does not contribute directly to ME180 cell growth but indirectly stimulates ME180 cell growth by inducing fibroblasts to produce HB-EGF. Fig. 6C also shows that dnEGFR expression in fibroblasts did not inhibit the enhanced proliferation of ME180 cells in coculture, confirming that EGFR ligands did not directly cause the activation of CCF or MEF cells.

In addition to the induced expression of HB-EGF by PDGF, HB-EGF also enhanced PDGF expression in ME180 cells. As shown by Western blot analysis (Fig. 5C), PDGF-BB synthesis

Published OnlineFirst October 18, 2011; DOI:10.1158/0008-5472.CAN-11-0034

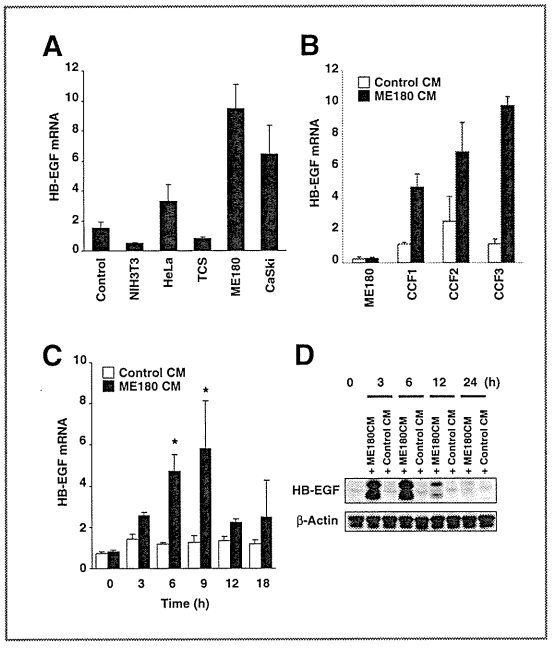

Figure 4. Induction of HB-EGF by cervical cancer cell CM. A, CM from the indicated cell lines or CCF1 cells (control) were added to CCF1 cells and incubated for 6 hours. HB-EGF mRNA expression in CCF1 cells was measured by real-time quantitative reverse transcriptase PCR. B, CM from ME180 cells or fresh medium (control) were added to CCF or ME180 cells and incubated for 6 hours. C, time course of HB-EGF mRNA upregulation. CM from CCF1 cells was used as a control. Bars show the mean ± SD for triplicate determinations. D, Western blotting detection of HB-EGF in CCF1 cells. CCF1 cells were incubated with CM from ME180 cells or fresh medium (control) for the indicated times. HB-EGF in cell lysates was detected by Western blotting. CM from ME180 cells upregulated HB-EGF synthesis. β-Actin was used as an internal loading control. *, $P < 0.05$.

in ME180 cells was enhanced when HB-EGF was added to cultured ME180 cells. These results indicate that PDGF secreted by ME180 cells induced HB-EGF expression in CCF1 cells, whereas HB-EGF produced by CCF1 cells enhanced ME180 cell proliferation and PDGF production. Thus, ME180 cells and CCF cells stimulate one another reciprocally through PDGF and HB-EGF expression (Fig. 7).

Discussion

Elevated levels of EGFR are associated with a poor prognosis for patients with cervical cancer, suggesting that the EGFR signaling pathway plays an important role in cancer progression (30–32). Here, we focused on HB-EGF expression and its growth-promoting activity in cervical cancer cells. Immunohistochemical and laser microdissection analyses revealed that HB-EGF was expressed in cancer-associated stroma but not in cancer epithelial cells. HB-EGF accumulated in CAF cells proximal to the cancer invasion front, although other types of cells might also express HB-EGF. Therefore, we investigated the role of stromal HB-EGF in cancer cell growth using *in vitro* coculture assays. ME180 cell and CaSki-cell

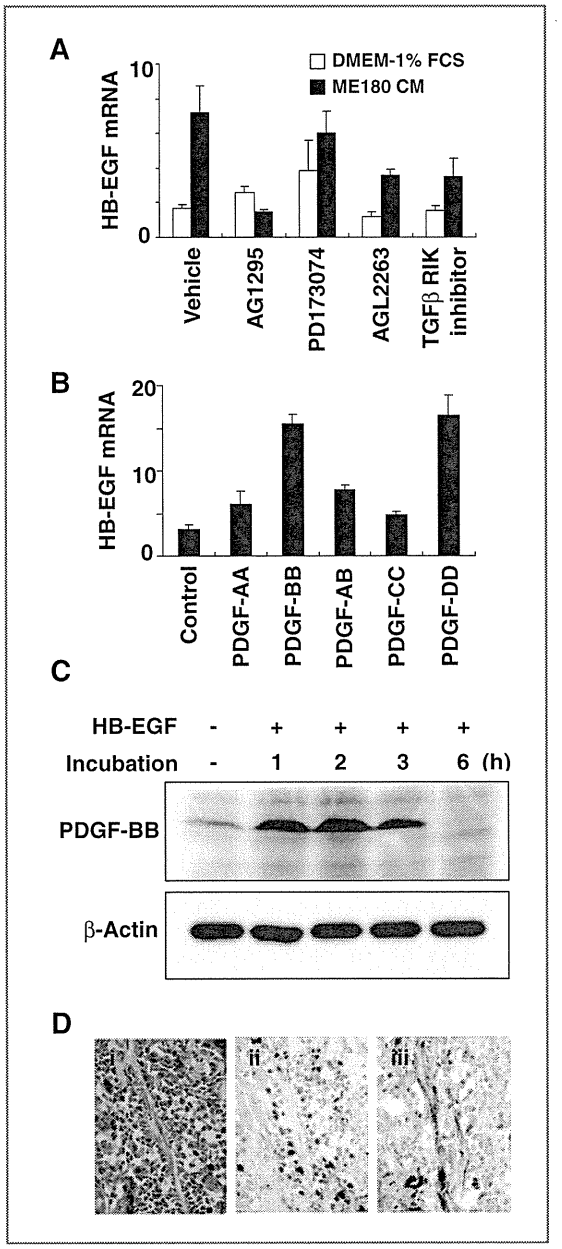

Figure 5. PDGF induces HB-EGF expression in CCF cells. A, CCF1 cells were incubated with fresh medium or CM from ME180 cells for 6 hours in the presence of PD173074 (2 μmol/L), AGL2263 (10 μmol/L), the TGFβ RI kinase (K) inhibitor II (1 μmol/L), or AG1295 (10 μmol/L). B, various subtypes of PDGF (5 ng/mL) were added to CCF1 cells and incubated for 6 hours. C, detection of PDGF-BB in ME180 cells by Western blotting. ME180 cells were incubated with or without HB-EGF (5 ng/mL) for the indicated periods, and cell lysates were subjected to immunoblotting. D, the tumors were dissected, and tissue sections were stained with an anti-PDGF-BB or anti-PDGFRβ antibody. Hematoxylin and eosin (H&E) staining (i), staining with an anti-PDGF-BB (ii), and anti-PDGFRβ antibody (iii). FCS, fetal calf serum.

Published OnlineFirst October 18, 2011; DOI:10.1158/0008-5472.CAN-11-0034

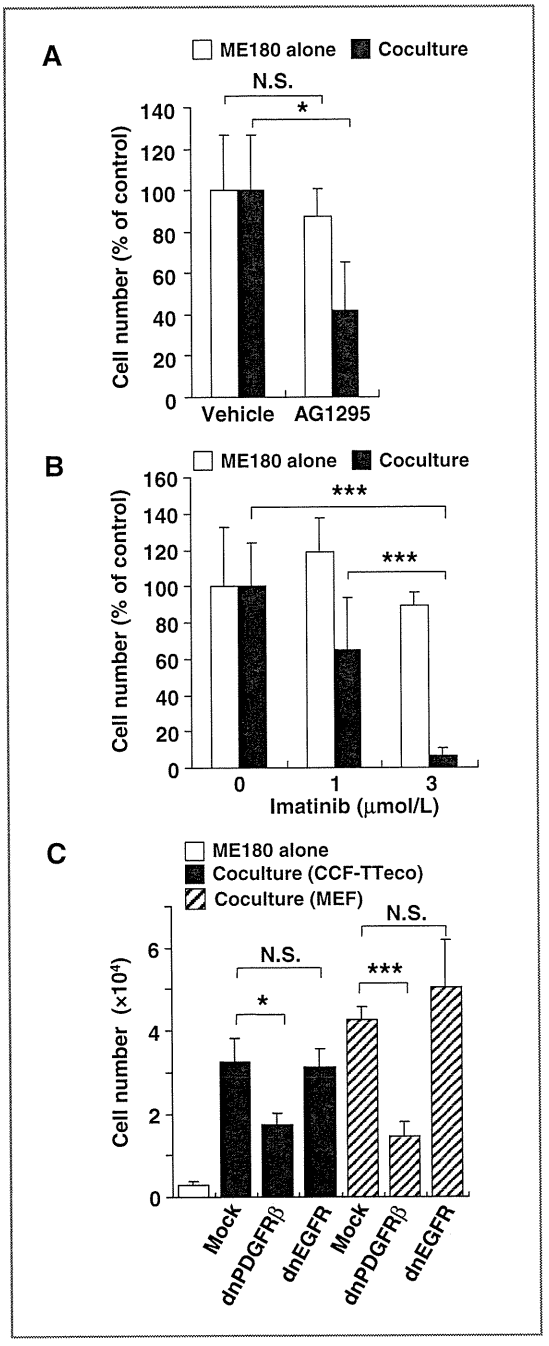

Figure 6. PDGFR inhibitors prevent enhanced proliferation of ME180 cells cocultured with CCF or MEF cells. A and B, AG1295 (A) and imatinib (B) inhibited ME180 cell proliferation in cocultures with CCF1 cells. ME180 cells were cocultured with CCF1 cells for 14 days in the presence of AG1295 (20 μmol/L; A) or imatinib at the indicated concentrations (B). C, ME180 cells (2×10^3) were cultured alone or with immortalized CCF1 (1×10^5) or MEF (1×10^5) cells infected with a control virus (mock), dnPDGFRβ-expressing virus, or dnEGFR-expressing virus for 1 week. *, $P < 0.05$; ***, $P < 0.005$.

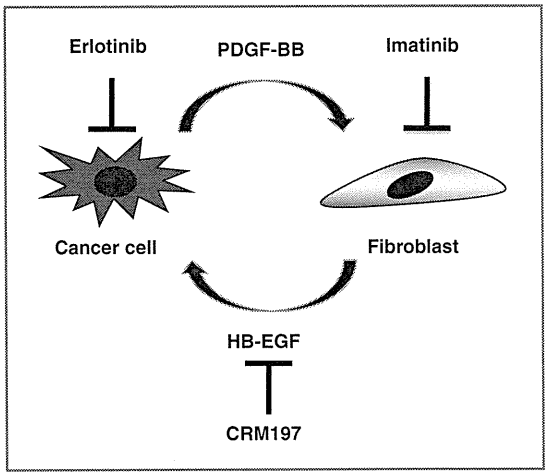

Figure 7. A model of cancer cell–stromal fibroblast interactions in the cervix. PDGF-BB produced by a cervical cancer cell upregulates HB-EGF through PDGFRβ activation in an adjacent fibroblast, which in turn facilitates cancer cell growth by activating EGFR. HB-EGF also induces PDGF synthesis in the cervical cancer cell. The paracrine loop can be blocked with inhibitors.

proliferation was greatly enhanced in the presence of CCF cells. An anti-HB-EGF–neutralizing antibody or CRM197 inhibited these effects. CRM197 not only inhibits the mitogenic activity of HB-EGF but also prevents its protein synthesis in cells that express high levels of pro-HB-EGF (33). No effects were observed on protein synthesis in CCF1 cells and ME180 cells at the concentration of CRM197 used here. Growth promotion of ME180 cells was also observed by coculture with MEF-HB$^{+/+}$ cells but not with MEF-HB$^{-/-}$ cells. Thus, HB-EGF expressed in CCF or MEF cells promoted ME180 cell proliferation in this coculture system. To the best of our knowledge, this is the first report that HB-EGF expressed in CAF promotes epithelial cancer cell growth.

Coinjection of CCF cells with ME180 cells enhanced tumor formation by ME180 cells in an athymic nude mouse model. Similarly, MEF-HB$^{+/+}$ cells enhanced the proliferation of ME180 cells much more than MEF-HB$^{-/-}$ cells. These results indicate that HB-EGF expressed in stromal cells enhances cancer cell growth *in vivo*, consistent with the results of our coculture assays. However, as HB-EGF is known to be involved in tumor angiogenesis (34, 35), the growth-enhancing effect of CCF or MEF cells *in vivo* might have been partly caused by the indirect growth-promoting effect of HB-EGF via neovascularization.

Another point we stress is that cervical cancer cells can produce a factor that induces HB-EGF synthesis in fibroblasts. Because PDGF is expressed in cervical cancer cells, we suspect that it is a candidate, although other factors may also contribute to this process. PDGF did not induce cancer cell growth itself but induced HB-EGF synthesis in CCF cells. Consequently, AG1295 and imatinib inhibited tumor growth by ME180 cells cocultured with CCF cells. Interestingly, addition of HB-EGF to ME180 cells in the absence of fibroblasts

Published OnlineFirst October 18, 2011; DOI:10.1158/0008-5472.CAN-11-0034

resulted in increased PDGF production. These results indicate that cancer epithelial cells and stromal fibroblasts interact reciprocally through PDGF and HB-EGF to form a positive feedback loop. PDGF ligands produced by cancerous epithelial cells stimulate the PDGFR-expressing stroma to upregulate the synthesis of FGFs, thereby promoting angiogenesis and epithelial-cell proliferation in a genetically-engineered mouse model (5). Therefore, not just a single growth factor system, but multiple systems could contribute to cancer–stroma interactions in cervical cancers.

Immunohistochemistry indicated that HB-EGF was localized at the stromal region proximal to the invasion front of cancerous epithelia. HB-EGF enhances cell motility as well as cell proliferation (11, 36), suggesting that HB-EGF contributes to the invasion and metastasis of cancerous epithelia. Membrane type 1 matrix metalloproteinase (MT1-MMP), which is involved in the degradation of ECM proteins, is believed to play an important role in cancer cell invasion and metastasis (37). MT1-MMP is expressed in cervical cancer cells, and its expression increases with cervical tumor progression (38). Invasion assays in collagen gel cultures showed that an EGF signal, in addition to MT1-MMP, is required for inducing keratinocyte invasiveness. We previously reported that MT1-MMP cleaves the N-terminal region of HB-EGF to convey enhanced mitogenic activity (39). Therefore, such processing of the N-terminal region of HB-EGF at the invasion front of cancer cells by MT1-MMP could be a cause of cervical cancer invasion.

There are several reports indicating a positive correlation between HB-EGF expression and cancer progression (24, 40, 41). In most of these cases, HB-EGF was upregulated in cancerous cells. Here, we showed that HB-EGF is produced in CAF and does not originate from cancer cells. The CAF-produced HB-EGF enhanced cancer cell proliferation. There is a report that HB-EGF plays a role in tumor progression in pericytes in a mouse model of pancreatic neuroendocrine tumorigenesis (35). Therefore, HB-EGF might contribute to cancer progression by various means. Although the development of therapeutic strategies targeting HB-EGF is only beginning, the combination of an HB-EGF inhibitor with other therapeutic agents, including PDGF inhibitors or MT1-MMP inhibitors, could lead to effective treatments for patients with refractory cancers.

Disclosure of Potential Conflicts of Interest

No potential conflicts of interest were disclosed.

Grant Support

This work was supported by Grants-in-Aid from the Ministry of Education, Culture, Sports, Science and Technology of Japan (16790950 to Y. Ueda, 17014057 to T. Enomoto, and 18591832 and 23240126 to E. Mekada).

The costs of publication of this article were defrayed in part by the payment of page charges. This article must therefore be hereby marked *advertisement* in accordance with 18 U.S.C. Section 1734 solely to indicate this fact.

Received January 7, 2011; revised August 29, 2011; accepted August 29, 2011; published OnlineFirst October 18, 2011.

References

1. Mueller MM, Fusenig NE. Friends or foes - bipolar effects of the tumour stroma in cancer. Nat Rev Cancer 2004;4:839–49.
2. Bhowmick NA, Neilson EG, Moses HL. Stromal fibroblasts in cancer initiation and progression. Nature 2004;432:332–7.
3. Kalluri R, Zeisberg M. Fibroblasts in cancer. Nat Rev Cancer 2006; 6:392–401.
4. Orimo A, Gupta PB, Sgroi DC, Arenzana-Seisdedos F, Delaunay T, Naeem R, et al. Stromal fibroblasts present in invasive human breast carcinomas promote tumor growth and angiogenesis through elevated SDF-1/CXCL12 secretion. Cell 2005;121:335–48.
5. Pietras K, Pahler J, Bergers G, Hanahan D. Functions of paracrine PDGF signaling in the proangiogenic tumor stroma revealed by pharmacological targeting. PLoS Med 2008;5:e19.
6. Ferlay J, Bray F, Pisani P, Parkin DM. Cancer incidence, mortality, and prevalence worldwide, version 2.0. Lyon, France: IARC; 2004.
7. zur Hausen H. Papillomaviruses and cancer: from basic studies to clinical application. Nat Rev Cancer 2002;2:342–50.
8. Gius D, Funk MC, Chuang EY, Feng S, Huettner PC, Nguyen L, et al. Profiling microdissected epithelium and stroma to model genomic signatures for cervical carcinogenesis accommodating for covariates. Cancer Res 2007;67:7113–23.
9. Higashiyama S, Abraham JA, Miller J, Fiddes JC, Klagsbrun M. A heparin-binding growth factor secreted by macrophage-like cells that is related to EGF. Science 1991;251:936–9.
10. Goishi K, Higashiyama S, Klagsbrun M, Nakano N, Umata T, Ishikawa M, et al. Phorbol ester induces the rapid processing of cell surface heparin-binding EGF-like growth factor: conversion from juxtacrine to paracrine growth factor activity. Mol Biol Cell 1995;6:967–80.
11. Higashiyama S, Abraham JA, Klagsbrun M. Heparin-binding EGF-like growth factor stimulation of smooth muscle cell migration: dependence on interactions with cell surface heparan sulfate. J Cell Biol 1993;122:933–40.
12. Raab G, Klagsbrun M. Heparin-binding EGF-like growth factor. Biochim Biophys Acta 1997;1333:F179–99.
13. Mizushima H, Wang X, Miyamoto S, Mekada E. Integrin signal masks growth-promotion activity of HB-EGF in monolayer cell cultures. J Cell Sci 2009;122:4277–86.
14. Miyamoto S, Hirata M, Yamazaki A, Kageyama T, Hasuwa H, Mizushima H, et al. Heparin-binding EGF-like growth factor is a promising target for ovarian cancer therapy. Cancer Res 2004;64:5720–7.
15. Ito Y, Higashiyama S, Takeda T, Yamamoto Y, Wakasa KI, Matsuura N. Expression of heparin-binding epidermal growth factor-like growth factor in pancreatic adenocarcinoma. Int J Pancreatol 2001;29:47–52.
16. Inui Y, Higashiyama S, Kawata S, Tamura S, Miyagawa J, Taniguchi N, et al. Expression of heparin-binding epidermal growth factor in human hepatocellular carcinoma. Gastroenterology 1994;107:1799–804.
17. Ito Y, Takeda T, Higashiyama S, Sakon M, Wakasa KI, Tsujimoto M, et al. Expression of heparin binding epidermal growth factor-like growth factor in hepatocellular carcinoma: an immunohistochemical study. Oncol Rep 2001;8:903–7.
18. Naef M, Yokoyama M, Friess H, Buchler MW, Korc M. Co-expression of heparin-binding EGF-like growth factor and related peptides in human gastric carcinoma. Int J Cancer 1996;66:315–21.
19. Ito Y, Higashiyama S, Takeda T, Okada M, Matsuura N. Bimodal expression of heparin-binding EGF-like growth factor in colonic neoplasms. Anticancer Res 2001;21:1391–4.
20. Thogersen VB, Sorensen BS, Poulsen SS, Orntoft TF, Wolf H, Nexo E. A subclass of HER1 ligands are prognostic markers for survival in bladder cancer patients. Cancer Res 2001;61:6227–33.
21. Ito Y, Takeda T, Higashiyama S, Noguchi S, Matsuura N. Expression of heparin-binding epidermal growth factor-like growth factor in breast carcinoma. Breast Cancer Res Treat 2001;67:81–5.
22. Wang YD, De Vos J, Jourdan M, Couderc G, Lu ZY, Rossi JF, et al. Cooperation between heparin-binding EGF-like growth factor and

Published OnlineFirst October 18, 2011; DOI:10.1158/0008-5472.CAN-11-0034

interleukin-6 in promoting the growth of human myeloma cells. Oncogene 2002;21:2584–92.
23. Tanaka Y, Miyamoto S, Suzuki SO, Oki E, Yagi H, Sonoda K, et al. Clinical significance of heparin-binding epidermal growth factor-like growth factor and a disintegrin and metalloprotease 17 expression in human ovarian cancer. Clin Cancer Res 2005;11:4783–92.
24. Miyamoto S, Yagi H, Yotsumoto F, Kawarabayashi T, Mekada E. Heparin-binding epidermal growth factor-like growth factor as a novel targeting molecule for cancer therapy. Cancer Sci 2006;97:341–7.
25. Gao K, Dai DL, Martinka M, Li G. Prognostic significance of nuclear factor-{kappa}B p105/p50 in human melanoma and its role in cell migration. Cancer Res 2006;66:8382–8.
26. Wang X, Mizushima H, Adachi S, Ohishi M, Iwamoto R, Mekada E. Cytoplasmic domain phosphorylation of heparin-binding EGF-like growth factor. Cell Struct Funct 2006;31:15–27.
27. Hamaoka M, Chinen I, Murata T, Takashima S, Iwamoto R, Mekada E. Anti-human HB-EGF monoclonal antibodies inhibiting ectodomain shedding of HB-EGF and diphtheria toxin binding. J Biochem 2010;148:55–69.
28. Mitamura T , Higashiyama S, Taniguchi N, Klagsbrun M, Mekada E. Diphtheria toxin binds to the epidermal growth factor (EGF)-like domain of human heparin-binding EGF-like growth factor/diphtheria toxin receptor and inhibits specifically its mitogenic activity. J Biol Chem 1995;270:1015–9.
29. Mori S, Heldin CH, Claesson-Welsh L. Ligand-induced polyubiquitination of the platelet-derived growth factor β-receptor. J Biol Chem 1992;267:6429–34.
30. Kim YT, Park SW, Kim JW. Correlation between expression of EGFR and the prognosis of patients with cervical carcinoma. Gynecol Oncol 2002;87:84–9.
31. Nicholson RI, Gee JM, Harper ME. EGFR and cancer prognosis. Eur J Cancer 2001;37:S9–15.
32. Noordhuis MG, Eijsink JJ, Ten Hoor KA, Roossink F, Hollema H, Arts HJ, et al. Expression of epidermal growth factor receptor (EGFR) and activated EGFR predict poor response to (chemo) radiation and survival in cervical cancer. Clin Cancer Res 2009;15:7389–97.
33. Kageyama T, Ohishi M, Miyamoto S, Mizushima H, Iwamoto R, Mekada E. Diphtheria toxin mutant CRM197 possesses weak EF2-ADP-ribosyl activity that potentiates its anti-tumorigenic activity. J Biochem 2007;142:95–104.
34. Ichise T, Adachi S, Ohishi M, Ikawa M, Okabe M, Iwamoto R, et al. Humanized gene replacement in mice reveals the contribution of cancer stroma-derived HB-EGF to tumor growth. Cell Struct Funct 2010;35:3–13.
35. Nolan-Stevaux O, Truitt MC, Pahler JC, Olson P, Guinto C, Lee DC, et al. Differential Contribution to Neuroendocrine Tumorigenesis of Parallel Egfr Signaling in Cancer Cells and Pericytes. Genes Cancer 2010;1:125–41.
36. Mine N, Iwamoto R, Mekada E. HB-EGF promotes epithelial cell migration in eyelid development. Development 2005;132:4317–26.
37. Itoh Y, Seiki M. MT1-MMP: a potent modifier of pericellular microenvironment. J Cell Physiol 2006;206:1–8.
38. Zhai Y, Hotary KB, Nan B, Bosch FX, Munoz N, Weiss SJ, et al. Expression of membrane type 1 matrix metalloproteinase is associated with cervical carcinoma progression and invasion. Cancer Res 2005;65:6543–50.
39. Koshikawa N, Mizushima H, Minegishi T, Iwamoto R, Mekada E, Seiki M. Membrane type 1-matrix metalloproteinase cleaves off the NH2-terminal portion of heparin-binding epidermal growth factor and converts it into a heparin-independent growth factor. Cancer Res 2010;70:6093–103.
40. Bos PD, Zhang XH, Nadal C, Shu W, Gomis RR, Nguyen DX, et al. Genes that mediate breast cancer metastasis to the brain. Nature 2009;459:1005–9.
41. Hoffmann AC, Danenberg KD, Taubert H, Danenberg PV, Wuerl P. A three-gene signature for outcome in soft tissue sarcoma. Clin Cancer Res 2009;15:5191–8.

Gynecologic Oncology 123 (2011) 241–247

Contents lists available at ScienceDirect

Gynecologic Oncology

journal homepage: www.elsevier.com/locate/ygyno

Radical hysterectomy with adjuvant radiotherapy versus definitive radiotherapy alone for FIGO stage IIB cervical cancer

Seiji Mabuchi [a,*,1], Mika Okazawa [c,1], Fumiaki Isohashi [b], Koji Matsuo [d], Yukinobu Ohta [c], Osamu Suzuki [e], Yasuo Yoshioka [b], Takayuki Enomoto [a], Shoji Kamiura [c], Tadashi Kimura [a]

[a] Department of Obstetrics and Gynecology, Osaka University Graduate School of Medicine, 2-2 Yamadaoka, Suita, Osaka, 565-0871, Japan
[b] Radiation Oncology, Osaka University Graduate School of Medicine, 2-2 Yamadaoka, Suita, Osaka, 565-0871, Japan
[c] Department of Gynecology, Osaka Medical Center for Cancer and Cardiovascular Diseases, 1-3-3 Nakamichi, Higashinari-ku, Osaka 537-8511, Japan
[d] Division of Gynecologic Oncology, Los Angeles County Medical Center, University of Southern California. 2020 Zonal Avenue, Los Angeles, CA 90031, USA
[e] Radiation Oncology, Osaka Medical Center for Cancer and Cardiovascular Diseases, 1-3-3 Nakamichi, Higashinari-ku, Osaka 537-8511,7 Japan

ARTICLE INFO

Article history:
Received 9 May 2011
Accepted 7 July 2011
Available online 6 August 2011

Keywords:
Cervical cancer
Radical hysterectomy
Definitive radiotherapy
FIGO stage IIB
Survival

ABSTRACT

Objectives. The aim of this study was to compare the treatment outcomes and adverse effects of radical hysterectomy followed by adjuvant radiotherapy with definitive radiotherapy alone in patients with FIGO stage IIB cervical cancer.

Methods. We retrospectively reviewed the medical records of FIGO stage IIB cervical cancer patients who were treated between April 1996 and December 2009. During the study period, 95 patients were treated with radical hysterectomy, all of which received adjuvant radiotherapy (surgery-based group). In addition, 94 patients received definitive radiotherapy alone (RT-based group). The recurrence rate, progression-free survival (PFS), overall survival (OS), and treatment-related complications were compared between the two groups.

Results. Radical hysterectomy followed by adjuvant radiotherapy resulted in comparable recurrence (44.2% versus 41.5%, $p=0.77$), PFS (log-rank, $p=0.57$), and OS rates (log-rank, $p=0.41$) to definitive radiotherapy alone. The frequencies of acute grade 3–4 toxicities were similar between the two groups (24.2% versus 24.5%, $p=1.0$), whereas the frequencies of grade 3–4 late toxicities were significantly higher in the surgery-based group than in the RT-based group (24.1% versus 10.6%, $p=0.048$). Cox multivariate analyses demonstrated that treatment with surgery followed by adjuvant radiotherapy was associated with an increased risk of grade 3–4 late toxicities, although the statistical significance of the difference was marginal (odds ratio 2.41, 95%CI 0.97–5.99, $p=0.059$).

Conclusions. Definitive radiotherapy was found to be a safer approach than radical hysterectomy followed by postoperative radiotherapy with less treatment-related complications and comparable survival outcomes in patients with FIGO stage IIB cervical cancer.

Introduction

Early stage cervical cancer (FIGO stage IB1–IIA) has been effectively treated with radical hysterectomy or definitive radiotherapy with similar survival outcomes [1–3]. In previous observational studies and a randomized controlled trial, the 5-year survival rate of patients with FIGO stage IB1–IIA cervical cancer treated with radical surgery was reported to range from 83 to 91%, which is comparable to the 74–91% reported for those treated with radiotherapy alone [1–3].

One of the advantages of primary surgery is that it allows the ovaries to be preserved and avoids early menopause. Primary surgery may result in less shortening and fibrosis of the vagina compared with definitive radiotherapy [1,4,5]. Another advantage of primary surgery is that it avoids the long-term complications of radiotherapy in patients who do not require postoperative adjuvant radiotherapy.

The advantage of definitive radiotherapy is that it can be administered to obese elderly patients and patients with coexisting diseases for which a surgical approach is usually contraindicated. Definitive radiotherapy also avoids the risks associated with anesthesia, as well as the risk of mortality and morbidity associated with surgery [4,5].

FIGO stage IIB cervical cancer is recognized as a locally advanced disease. The National Comprehensive Cancer Network (NCCN) guidelines recommend cisplatin-based chemoradiotherapy as the primary treatment for FIGO stage IIB disease [6]. According to a previous FIGO annual report, 72% of patients with FIGO stage IIB cervical cancer were

* Corresponding author at: Department of Obstetrics and Gynecology, Osaka University Graduate School of Medicine. 2-2 Yamadaoka, Suita, Osaka 565-0871, Japan. Fax: +81 6 6879 3359.
E-mail address: smabuchi@gyne.med.osaka-u.ac.jp (S. Mabuchi).
[1] These authors contributed equally to this work.

0090-8258/$ – see front matter © 2011 Elsevier Inc. All rights reserved.
doi:10.1016/j.ygyno.2011.07.009

treated with definitive radiotherapy [7]. However, in Japan, the majority of patients with FIGO stage IIB cervical cancer have been subjected to radical hysterectomy, and only patients who declined surgery and those with coexisting medical conditions have been treated with definitive radiotherapy. In a previous report from the Japan Society of Obstetrics and Gynecology (JSOG), 62.7% of FIGO stage IIB cervical cancer patients received surgery-based therapy [4,8].

In the aforementioned FIGO annual report, the 5-year survival rate of 232 FIGO stage IIB cervical cancer patients who were treated with surgery followed by adjuvant radiotherapy was 64.3%, which was comparable to the 64.2% observed in 1718 patients treated with definitive radiotherapy and the 64.4% observed in 112 patients treated with concurrent chemoradiotherapy (CCRT) [7]. Previous retrospective investigations showing the similar survival outcomes of the two treatment modalities suggest that there is no definitive consensus for the treatment of choice for patients with FIGO stage IIB cervical cancer [7,9,10]. However, treatment-related complications, which may inversely affect the patient's quality of life after cancer therapy are a crucial consideration when deciding between two treatment modalities with equivalent survival outcomes. As combined treatment with radical hysterectomy plus adjuvant radiotherapy is associated with significantly increased morbidity compared with surgical treatment alone [11,12], definitive treatment with radiotherapy alone may be beneficial for FIGO stage IIB cervical cancer patients who usually require adjuvant radiotherapy after radical hysterectomy.

Due to the lack of randomized controlled trials comparing these two treatment modalities, we are unable to determine which treatment option is superior for FIGO stage IIB cervical cancer patients at this point. Therefore, we retrospectively compared radical hysterectomy plus postoperative radiotherapy with definitive radiotherapy alone with regard to survival and treatment-related complications in patients with FIGO stage IIB cervical cancer.

Materials and methods

Patients

Approval for the data acquisition and analysis was obtained from the Institutional Review Board of Osaka University Hospital and Osaka Medical Center for Cancer and Cardiovascular Diseases. A list of patients who were treated for FIGO stage IIB cervical cancer from April 1996 to December 2009 was generated from each institutional tumor registry. Then, patients who were treated with either radical hysterectomy combined with adjuvant radiotherapy (surgery-based group, n = 108) or definitive radiotherapy alone (RT-based group, n = 94) were identified through a chart review, and their clinical information was retrospectively reviewed. The patients were clinically staged according to the FIGO staging system without general anesthesia. The pretreatment work-up consisted of (i) an investigation of the patient's complete medical history and a physical examination; (ii) a laboratory evaluation including a complete blood count and biochemistry panels; and (iii) radiological evaluations including a chest X-ray, computed tomography (CT) of the abdomen and pelvis, and magnetic resonance imaging (MRI). Intravenous pyelogram, cystoscopy, and rectosigmoidoscopy were considered optional. Lymph nodes measuring 10 mm or greater across their largest diameter on CT or MRI were defined as metastatic nodes. Patients who had radiologic evidences of paraaortic lymph nodes (PALN) or supraclavicular lymph nodes metastasis were excluded from the analysis. Of the 108 patients in the surgery-based group, 64 were included in previous studies [13,14].

Treatments

Surgery

All the patients in the surgery-based group were treated with radical hysterectomy (type III) and pelvic lymphadenectomy. The lymphadenectomy procedure included complete bilateral pelvic lymphadenectomy with the aim of removing all of the external iliac, internal iliac, common iliac, obturator, suprainguinal, and presacral lymph nodes.

Adjuvant radiotherapy

In our institutions, postoperative radiotherapy was indicated when a patient's pathological report displayed any one of the following "high-risk" prognostic factors: parametrial invasion, pelvic lymph nodes metastases, or a positive margin in the hysterectomy specimen, or the following "intermediate-risk" prognostic factors: deep stromal invasion, lymphovascular space involvement, or a tumor size of 4 cm or greater.

The patients were treated with external beam whole pelvic radiotherapy plus concurrent platinum-based chemotherapy as reported previously [13,14]. The patients who refused the use of concurrent chemotherapy or who developed cervical cancer before the introduction of CCRT were treated with pelvic radiotherapy alone. Eighteen patients whose pathological reports revealed multiple pelvic node metastases were treated with extended field radiotherapy (EFRT) without concurrent chemotherapy, as reported previously [14,15].

External beam radiotherapy (EBRT) was delivered from a linear accelerator using the anteroposterior parallel opposing technique in the settings of adjuvant therapy and definitive radiotherapy. The superior margin of the external radiation field was located at the top of the fifth lumber vertebra, and the inferior border of the obturator foramen was used as the inferior margin. Laterally, the field extended 2 cm beyond the lateral margin of the bony pelvic wall. We used multi-leaf collimators to block the upper and lower corners of the radiation field [13]. The external irradiation was delivered to the whole pelvis at 2 Gy per fraction in 5 fractions per week, for a total of 23 or 25 fractions (46 Gy or 50 Gy).

The radiation field encompassed the pelvic and PALN drainage areas. The superior margin of the PALN area was located at the bottom of the T12 vertebral body, and the inferior margin was located at the inferior border of the obturator foramen. The lateral margin was located 2 cm lateral of the widest margin of the bony pelvis [14]. The external irradiation was delivered to the EFRT fields for a total of 45 Gy in 25 fractions, and to the whole pelvis at 1.8 Gy per fraction, for a total of 28 fractions (50.4 Gy).

Ten patients that displayed vaginal invasion close to the surgical margin received intracavitary radiotherapy (ICRT).

Definitive radiotherapy

The definitive radiotherapy consisted of pelvic external beam radiotherapy (EBRT) plus concurrent chemotherapy followed by high dose rate intracavitary brachytherapy (HDR-ICBT), as reported previously [16]. The external irradiation was delivered to the whole pelvis at 2 Gy per fraction for 5 fractions per week, for a total of 25 fractions (50 Gy). The pelvic radiation field was the same as that employed for the adjuvant radiotherapy, but extended inferiorly in cases involving vaginal invasion. A midline block (width at the midline: 4 cm) was inserted into the lower central two-thirds of the pelvic field after 30 Gy had been delivered. After adequate tumor regression, HRD-ICBT was performed once a week during the course of the EBRT using the centrally shielded field. Usually, the first HDR-ICBT was applied after 30 Gy of EBRT. ICBT was administered to the patients using a microSelectron HDR (Nucletron, Veenendaal, The Netherlands). Vaginal packing was used to maximize the distances from the source to the bladder wall and the rectal wall. The ICBT dose was prescribed at Point A, which was defined as 2 cm above the cervical os marker and 2 cm perpendicular to the uterine axis along the plane of the uterus. The total planned dose for the HDR-ICBT was 28.8 or 30 Gy in four fractions.

Concurrent chemotherapy

In our institutions, nedaplatin has been employed as a radiosensitizing agent for patients with cervical cancer [13,14,16]. Nedaplatin was given intravenously weekly or biweekly during the course of pelvic EBRT, as reported previously in the settings of adjuvant radiotherapy and definitive radiotherapy [13,14,16].

Follow-up

The patients were followed-up regularly by both gynecologic oncologists and radiation oncologists as reported previously [17]. When recurrence was suspected, a biopsy was taken for confirmation whenever possible. The median duration of follow-up was 44 months (range: 6–168 months) in the surgery-based group, and 60 months (range: 4–154 months) in the RT-based group.

Toxicity

Adverse effects that occurred within 90 days of the start of the primary treatment were considered to be acute complications, and those that occurred 90 days or later after the start of treatment were considered to be late complications. The severity of acute and late complications was classified according to the NCI Cancer Therapy Evaluation Program Common Terminology Criteria for Adverse Events (CTCAE), Version 2.0.

Statistical analysis

The differences between the two groups with respect to categorical variables such as clinical stage, histology, parametrial involvement, deep stromal invasion, and surgical margin status were assessed with Fisher's exact test, and odds ratios and 95% confidence intervals (95%CI) were determined. Continuous variables such as age, maximum tumor diameter, and the duration of radiotherapy were analyzed with the Mann Whitney *U* test. Pretreatment hemoglobin levels were compared using the Student's *t* test. Treatment related toxicities were compared with Fisher's exact test. Survival curves were computed using the Kaplan–Meier method, and the statistical significance of differences in survival was determined with the Log-rank test. Progression-free survival (PFS) was defined as the time interval between the initial diagnosis and the detection of recurrence. Overall survival (OS) was defined as the time interval between the initial diagnosis and death or the latest observation. Multivariate analysis of the significance of treatment modality was performed with the logistic regression test for late adverse effect (expressed as the odds ratio and 95%CI) and the Cox regression test for survival outcomes (expressed as the hazard ratio and 95%CI), respectively. Intention-to-treat analysis was separately performed based on the initial allocation of surgery with adjuvant radiotherapy versus definitive radiotherapy alone. All statistical analyses were two-tailed, and p-values of less than 0.05 were considered statistically significant. The Statistical Package for Social Scientists (SPSS, version 18.0, IL) was used for all the analyses.

Results

Patient characteristics

Among the 202 patients in the two groups who were eligible for the retrospective analysis, 95 were treated with radical hysterectomy combined with adjuvant chemoradiotherapy or radiotherapy according to their pathological risk factors (surgery-based group) and 94 were treated with definitive radiotherapy or chemoradiotherapy alone (RT-based group). The remaining 13 (6.4%) patients underwent surgical treatment and displayed pathological risk factors; however, they declined postoperative adjuvant radiotherapy (suboptimal treatment group). We therefore analyzed a total of 189 patients in the surgery-based group and RT-based group (Table 1). The suboptimal treatment group was subsequently investigated in separate analyses (intention-to-treat analysis), and the results are shown in the supplemental tables and figures.

As shown in Table 1, in the surgery-based group, the mean age of the patients was 51 years. Seventy-six patients (80%) had SCC, and 18 (20%) displayed non-SCC histology. The median tumor diameter was 40 mm. Fifty patients (52.6%) received postoperative concurrent chemoradiotherapy (CCRT). Eleven patients (11.6%) showed radiologic evidence of lymphadenopathy, and 53 patients (55.8%) showed histological evidence of pelvic node metastases. Among the 95 patients in the surgery-based group, 81 displayed pathological evidence of parametrial involvement (14 were false positives). Thus, the positive predictive value of pelvic examination for detecting parametrial invasion was 85.3%.

In the RT-based group, the mean age of the patients was 63 years. Eighty-two patients (87.2%) had SCC, and 18 (12.8%) had non-SCC histology. The median tumor diameter was 44 mm. Thirty-four patients (36.2%) were treated with CCRT. Twenty-six patients (27.7%) showed radiologic evidence of lymphadenopathy.

When the surgery-based group was compared with the RT-based group, there were no statistically significant differences in terms of histological distribution, tumor diameter, or the pretreatment hemoglobin level. However, the patients in the surgery-based group were significantly younger than those in the RT-based group ($P<0.001$). In addition, radiological evidence of lymphadenopathy was more frequently observed in the RT-based group than in the surgery-based group ($p=0.006$).

Treatment outcome

As shown in Table 2, during the follow-up period, recurrence was observed in 42 patients (44.2%) in the surgery-based group and 39 patients (41.5%) in the RT-based group. In the surgery-based group, 14 patients developed recurrence in the pelvis, 18 developed recurrence in distant areas outside of the pelvis, and 10 patients developed recurrence in both pelvic and distant areas. In the RT-based

Table 1
Patient characteristics.

		Surgery + RT	Radiotherapy	P-value
Number of patients		n=95	n=94	
Age	Mean (±SD)	51 (±11.2)	63 (±13.8)	P<0.001
Histology	SCC	76 (80%)	82 (87.2%)	p=0.47
	A or AS	18 (18.9%)	11 (11.7%)	
	Others	1 (1.1%)	1 (1.1%)	
Maximal tumor diameter*	Median (mm)	40 (20–100)	44 (10–80)	p=0.47
Primary treatment	Surgery** plus RT	45 (47.4%)	0	p<0.001
	Surgery** plus CCRT	50 (52.6%)	0	
	Definitive RT	0	60 (63.8%)	
	Definitive CCRT	0	34 (36.2%)	
Pelvic node involvement (Radiological evidence)	Yes	11 (11.6%)	26 (27.7%)	p=0.006
	No	84 (88.4%)	68 (72.3%)	
Pretreatment hemoglobin level***	Mean (mg/dl)	11.8 (±1.2)	12.2 (±1.5)	p=0.16

PORT, postoperative radiotherapy; RT, radiotherapy; CCRT, concurrent chemoradiotherapy; SCC, squamous cell carcinoma; A, adenocarcinoma; AS, adenosquamous carcinoma.

* The maximal tumor diameter was measured three-dimensionally based on T2-weighted images. The longest diameter was considered to represent the maximal tumor diameter.

** Radical hysterectomy (Type III) plus pelvic lymphadenectomy.

*** Hemoglobin level just before the start of radiotherapy.

Table 2
Treatment outcome.

		Surgery + RT	Radiotherapy	P-value
Number of patients		n = 95	n = 94	
Patients with recurrence	N (%)	42 (44.2%)	39 (41.5%)	p = 0.77
Site of recurrence	Pelvis	14 (14.7%)	12 (12.8%)	p = 0.57
	Pelvis plus distant	10 (10.5%)	5 (5.3%)	
	Distant	18 (18.9%)	22 (23.4%)	
Total deaths	N (%)	34 (35.8%)	33 (35.1%)	p = 0.64
	Disease	33 (34/7%)	30 (31.6%)	
	Other	1 (1.1%)	3 (3.2%)	

group, 12 patients developed recurrence in the pelvis, 22 patients developed recurrence in distant areas outside of the pelvis, and 5 patients developed recurrence in both pelvic and distant areas. The recurrence rate and pattern of recurrence did not differ between the two treatment groups ($p = 0.77$ and $p = 0.57$, respectively).

At the time of this report, 33 patients from the surgery-based group (34.7%) had died due to cervical cancer, and 1 patient (1.1%) had died due to another disease. In the RT-based group, 30 patients (31.6%) died due to cervical cancer, and 3 patients (3.2%) died due to other diseases. As shown in Fig. 1, although the surgery-based group showed slightly less pelvic recurrence and higher survival rates, the differences were not statistically significant; pelvic recurrence ($p = 0.25$), PFS (log-rank; $p = 0.57$), and OS rates (log-rank; $p = 0.41$). The estimated 5-year overall survival rate in the surgery-based group was 66.4%, which was comparable to the 68.3% observed in the RT-based group (Fig. 1). Similar results were obtained in the intention-to-treat analysis (Supplemental Fig. 1). As shown in Fig. 1, although the surgery group showed slightly higher survival rates, the difference was not statistically significant (PFS: $p = 0.24$; log-rank, OS: $p = 0.25$; log-rank). The pelvic recurrence rate was significantly lower in the RT-based group than in the surgery group (Supplemental Fig. 1C).

After controlling for other variables in the multivariate analysis, no significant difference in survival outcome was detected between the patients in the surgery-based group and those in the RT-based group (Table 3). Multivariate analysis also demonstrated that age, histology, tumor diameter, pelvic node metastasis, and the duration of radiotherapy were significant prognostic factors for both PFS and OS.

Similarly, in a multivariate analysis of the intention-to-treat groups, no significant difference in survival outcome was detected between the patients in the surgery group and those in the RT-based group (Supplemental Table 3).

Adverse effects

No treatment-related deaths were reported. Among the 95 patients in the surgery-based group, 23 (24.2%) patients suffered grade 3 or 4 acute toxicities: 18 patients had neutropenia and 2 patients developed small bowel obstruction (SBO), both of which were treated conservatively; one patient developed bladder perforation requiring urinary diversion; one patient had severe diarrhea; and one patient developed a large infected lymphocyst accompanied by serious pain (Table 4). Among the 94 patients who were treated with definitive radiotherapy, 23 patients (24.5%) suffered grade 3 or 4 acute toxicities: 21 patients developed neutropenia, one patient developed anemia, and one patient developed diarrhea. All reported

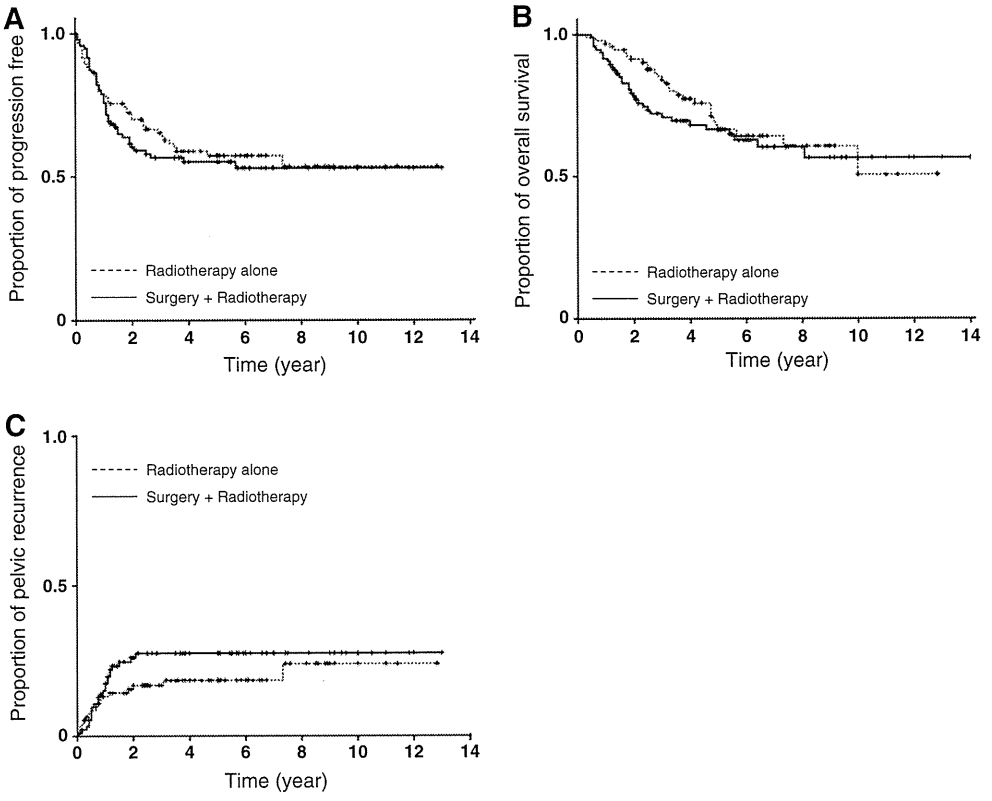

Fig. 1. A: Progression free survival among patients in the surgery-based group and RT-based group. The progression free survival rate in the surgery-based group was similar to that in the RT-based group (log-rank, $p = 0.57$). B: Overall survival in the surgery-based group and RT-based group. The overall survival rate in the surgery-based group was similar to that in the RT-based group (log-rank, $p = 0.41$). C: Cumulative pelvic recurrence rate among patients in the surgery-based group and RT-based group. The pelvic recurrence rate was similar among the two groups (log-rank, $p = 0.25$).

Table 3
Multivariate analysis for survival outcome.

	Progression-free survival		Overall survival	
	HR (95%CI)	P-value	HR (95%CI)	P-value
Age (>50 versus ≤50)	0.60 (.036–0.99)	0.046	0.57 (0.33–0.99)	p=0.045
Histology (SCC versus non-SCC)	0.55 (0.31–0.97)	0.039	0.64 (0.33–1.22)	p=0.17
Maximum tumor diameter (≥4 cm versus <4 cm)	1.83 (1.05–3.18)	0.032	1.39 (0.76–2.54)	p=0.28
Pelvic node metastasis (yes versus no)	3.33 (2.00–5.56)	<0.001	2.72 (1.53–4.83)	p<0.001
Pre-RT hemoglobin (<11 g/dL versus ≥11 g/dL)	0.91 (0.54–1.52)	0.72	0.83 (0.46–1.50)	p=0.53
RT duration (continuous)	1.03 (1.00–1.06)	0.041	1.04 (1.00–1.07)	p=0.023
Treatment (surgery + RT versus RT alone)	0.75 (0.44–1.25)	0.27	0.94 (0.52–1.68)	p=0.83

Cox proportional hazard regression test, HR: hazard ratio, 95%CI: 95% confidence interval, SCC: squamous cell carcinoma, RT: radiotherapy.

grade 3–4 acute toxicities were manageable with conservative treatment. The frequencies of acute grade 3–4 toxicities were similar between the two treatment groups (p=1.0).

Among a total of 189 patients, 31 patients (16.4%) developed grade 3–4 late toxicities. Of these, SBO and lymphedema were the two most common late toxicities. In the surgery-based group, grade 3–4 late toxicities were observed in 21 patients (22.1%). Eleven patients developed SBO (four were treated surgically and seven were treated conservatively). Five patients developed lymphedema, and one patient developed a large infected lymphocyst. Bladder dysfunction, bladder perforation, and hydronephrosis were observed in 1, 1, and 2 patients, respectively.

In the RT-based group, grade 3–4 late toxicities were observed in 10 patients (10.6%). One patient developed SBO 4 months after the completion of radiotherapy, which required surgical intervention. Lymphedema was observed in two patients. Small intestinal perforation, enterocolitis, and bone fractures were observed in 2, 3, and 2 patients, respectively.

Table 4
Grade 3–4 acute and late toxicities.

		Surgery + RT	Definitive RT	P-value
Number of patients		n=95	n=94	
Grade 3–4 acute toxicity	N (%)	23 (24.2%)	23 (24.5%)	p=1.0
	Neutropenia	18 (18.9%)	21 (22.3%)	
	Anemia	0	1 (1.1%)	
	Small bowel obstruction	2 (2.1%)	0	
	Diarrhea	1 (1.1%)	1 (1.1%)	
	Bladder perforation	1 (1.1%)	0	
	Lymphocyst	1 (1.1%)	0	
Grade 3–4 late toxicity	N (%)	21 (22.1%)	10 (10.6%)	p=0.048
	Small bowel obstruction	11 (11.6%)	1 (1.1%)	
	Small intestinal perforation	0	2 (2.1%)	
	Enterocolitis	0	3 (3.2%)	
	Bladder dysfunction	1 (1.1%)	0	
	Bladder perforation	1 (1.1%)	0	
	Hydronephrosis	2 (2.1%)	0	
	Lymphocyst	1 (1.1%)	0	
	Lymphedema	5 (5.3%)	2 (2.1%)	
	Fracture	0	2 (2.1%)	

RT, radiotherapy.

When the two groups were compared, the frequencies of late grade 3–4 toxicities were significantly higher in the surgery-based group than in the RT-based group (p=0.048).

As shown in Table 5, surgery-based therapy was associated with an increased risk of grade 3–4 late toxicities, although the statistical significance of the difference was marginal (odds ratio: 2.41, 95%CI: 0.97–5.99, p=0.059).

Similar results were obtained in the intention-to-treat analysis. The frequencies of grade 3–4 late toxicities were higher in the surgery group than in the RT-based group, although the statistical significance of the difference was marginal (p=0.056) (Supplemental Table 4). Moreover, in multivariate analysis, surgery-based therapy was associated with an increased risk of grade 3–4 late toxicities (odds ratio: 2.45, 95%CI: 1.03–5.86, p=0.043) (Supplemental Table 5).

Discussion

In previous observational studies, the 5-year survival rates of patients with FIGO stage IIB cervical cancer who were treated with radical surgery were reported to range from 64 to 69%, which is comparable to those treated with definitive radiotherapy (64–69%) [7,9]. Although these studies were retrospective, they indicate that radical surgery and definitive radiotherapy are equally efficacious for FIGO stage IIB cervical cancer in terms of survival outcome [7,9].

However, in the current study, the rate of severe late complications in the surgery-based group was significantly higher than that observed in the RT-based group (22.1% versus 10.6%, p=0.048). In our patients, SBO and lymphedema were the two most common late toxicities. The incidences of severe SBO and severe lymphedema in the two treatment groups were consistent with those of previous reports [9–12,18,19]. Most SBO and lymphedema in our patients developed in the first 4 years; however, one patient developed serious lymphedema 8 years after the completion of adjuvant radiotherapy. As previous reports suggested that both SBO [20] and lymphedema [21] can develop more than 10 years after the completion of adjuvant radiotherapy, patients should be informed about the lifelong risk of these complications before the initial surgery, and careful post-treatment follow-up is required to reduce the necessity of major interventions.

The risk factors for the development of severe late toxicities have been investigated in several retrospective studies [18–20,22]. In cervical cancer patients treated with radical hysterectomy, the addition of adjuvant radiotherapy, age, radiation dose fraction, and prior abdominal surgery has been reported to be risk factors for SBO

Table 5
Multivariate analysis for Grade 3–4 late adverse effects.

	Proportion (%)	Odds ratio (95%CI)	P-value
Age (>50 versus ≤50)	14.8 versus 21.3%	0.73 (0.29–1.82)	p=0.5
Histology (SCC versus non-SCC)	14.6 versus 25.8%	0.58 (0.22–1.55)	p=0.28
Maximum tumor diameter (≥4 cm versus <4 cm)	15.9 versus 17.5%	0.92 (0.38–2.25)	p=0.86
Pelvic node metastasis (yes versus no)	15.2 versus 17.3%	0.66 (0.27–1.62)	p=0.36
Pre-RT hemoglobin (<11 g/dL versus ≥11 g/dL)	16.7 versus 16.3%	1.14 (0.42–3.08)	p=0.8
RT duration (continuous)		0.99 (0.04–1.05)	p=0.8
Treatment (surgery + RT versus RT alone)	22.1 versus 10.6%	2.41 (0.97–5.99)	p=0.059
Early adverse effects (yes versus no)	10.9 versus 18.2%	0.53 (0.18–1.53)	p=0.24

Logistic regression test. 95%CI: 95% confidence interval, SCC: squamous cell carcinoma, and RT: radiation therapy.

[19,20,22]. The following predictive factors that increase the risk of severe lymphedema after radical hysterectomy have also been reported: adjuvant radiotherapy, age, the number of lymph nodes examined, and the patient's build [18]. In our study, surgery with adjuvant radiotherapy was the only factor associated with an increased risk of grade 3–4 late toxicity, although the statistical significance of this increase was marginal ($p=0.059$).

Patients with FIGO stage IIB cervical cancer usually exhibit high-risk pathological factors such as positive pelvic nodes, parametrial invasion, or a positive surgical margin; thus, postoperative adjuvant radiotherapy is inevitable in this population. Therefore, opting for definitive radiotherapy instead of radical surgery, especially in patients with the abovementioned risk factors for the development of severe late toxicities, will provide a better quality of life after the completion of treatment.

Considering the relatively high incidence of severe late complications observed in both treatment groups in the current study, further efforts need to be made to reduce the incidences of these complications. One possible strategy is the use of more conformal dose distributions with intensity-modulated radiation therapy (IMRT) [23]. Clinical trials of IMRT in the settings of adjuvant radiotherapy and definitive radiotherapy for stage IIB disease need to be conducted in the future.

In our patients, despite the intensive treatments administered, a significant number of patients still suffered recurrence and died of their disease in both the surgery-based and RT-based groups. Of a total of 189 patients in the surgery-based group or RT-based group, 27 developed PALN recurrence. Of these, 11 suffered an isolated PALN relapse. In the surgery-based group, all patients who developed PALN recurrence displayed evidence of pelvic node metastasis in pathological examinations of surgical specimens. The mean number of pelvic node metastases in patients who developed PALN recurrence was 2, which was significantly greater than the 1.28 observed in patients without PALN recurrence ($p=0.002$). In addition, the PALN recurrence rate in patients with pathological evidence of pelvic node metastasis was significantly higher than those without pathological evidence of pelvic node metastasis (25% versus 0%, $p=0.0015$). A similar result was obtained for patients in the RT-based group. The PALN recurrence rate in patients with radiological evidence of pelvic node metastasis was higher than those without radiological evidence of pelvic node metastasis, although the statistical significance of the difference was marginal (30.8% versus 10.3%, $p=0.07$). Collectively, these results indicate that radiological or pathological evidence of pelvic node metastasis is a promising indicator of PALN recurrence. To prevent this pattern of recurrence and eventually improve patient survival, novel treatments such as extended-field IMRT combined with concurrent chemotherapy need to be investigated in the settings of adjuvant and definitive radiotherapy for patients who are at high-risk of PALN recurrence in future clinical trials.

In the current study, age, tumor diameter, pelvic node involvement, and the duration of radiotherapy were identified as significant prognostic factors for survival (Table 3). Our results were consistent with those of previous investigations in which pelvic node status [9,24], parametrial involvement [9], and tumor size [25] were identified as prognostic factors for survival in patients with FIGO stage IIB cervical cancer. Thus, the development of new treatment strategies for patients with known risk factors for survival is urgently needed. For this purpose, novel treatments such as the use of new cytotoxic and/or biologic agents as radiosensitizers, the addition of consolidation chemotherapy after postoperative adjuvant radiotherapy or definitive radiotherapy should be investigated in future clinical trials.

The limitations of our study need to be addressed. Due to its retrospective nature, potential confounding biases may have been missed in the analysis, such as the selection bias introduced by physicians in determining which patients should be considered for radical surgery plus adjuvant radiotherapy. In our study, the patients in the surgery-based group were significantly younger and displayed less radiological evidence of pelvic node metastasis than those in the RT-based group, indicating that more patients with favorable prognoses were allocated to the surgery-based group than the RT-based group. There are several possible explanations for this. In our institutions, surgery is preferred for the treatment of younger cervical cancer patients with a concept of avoiding late radiation toxicities and reductions in sexual function. In addition, the choice of treatment might have been influenced by the specialty training of the surgeons, as reported in the USA [26]. Moreover, the educational level and/or the socio-economical status of the patients might also have affected the treatment selection. These potential biases can only be eliminated in a prospective randomized controlled study.

In conclusion, definitive radiotherapy is a safer approach than radical hysterectomy followed by postoperative radiotherapy; i.e., it is associated with less treatment-related complications and comparable survival outcomes, in patients with FIGO stage IIB cervical cancer. To convincingly demonstrate the superiority of surgical approaches in this patient population, the survival outcome, the frequency of treatment-related complications, and the patient's quality of life should be compared between the two treatment modalities in a randomized controlled trial.

Supplementary materials related to this article can be found online at doi:10.1016/j.ygyno.2011.07.009.

Conflict of interest statement
The authors declare that they have no conflicts of interest.

Acknowledgments

The authors thank the following colleagues who participated in this study: Kanji Masuhara, Kiyoshi Yoshino, Masami Fujita, Tateki Tsutsui, Shintaroh Maruoka, and Kinji Nishiyama.

References

[1] Landoni F, Maneo A, Colombo A, Placa F, Milani R, Perego P, et al. Randomised study of radical surgery versus radiotherapy for stage Ib–IIa cervical cancer. Lancet 1997;350:535–40.
[2] Morley GW, Seski JC. Radical pelvic surgery versus radiation therapy for stage I carcinoma of the cervix (exclusive of microinvasion). Am J Obstet Gynecol 1976;126:785–98.
[3] Perez CA, Camel HM, Kao MS, Hederman MA. Randomized study of preoperative radiation and surgery or irradiation alone in the treatment of stage IB and IIA carcinoma of the uterine cervix: final report. Gynecol Oncol 1987;27:129–40.
[4] Undurraga M, Loubeyre P, Dubuisson JB, Schneider D, Petignat P. Early-stage cervical cancer: is surgery better than radiotherapy? Expert Rev Anticancer Ther Mar 2010;10:451–60.
[5] Suprasert P, Srisomboon J, Kasamatsu T. Radical hysterectomy for stage IIB cervical cancer: a review. Int J Gynecol Cancer 2005;15:995–1001.
[6] National Comprehensive Cancer Network Clinical Practice Guidelines in Oncology, Cervical Cancer—v.1.2011. http://www.nccn.org/professionals/physician_gls/pdf/cervical.pdf.
[7] Benedet JL, Odicino F, Maisonneuve P, Beller U, Creasman WT, Heintz AP, et al. Carcinoma of the cervix uteri. Int J Gynaecol Obstet 2003;83(Suppl 1):41–78.
[8] Annual report from Cancer Registry Committee of Japan Society of Obstetrics and Gynecology. Acta Obstet Gynaecol Jpn 1983;35:737–52.
[9] Kasamatsu T, Onda T, Sawada M, Kato T, Ikeda S. Radical hysterectomy for FIGO stage IIB cervical cancer: clinicopathological characteristics and prognostic evaluation. Gynecol Oncol 2009;114:69–74.
[10] Yamashita H, Okuma K, Kawana K, Nakagawa S, Oda K, Yano T, et al. Comparison between conventional surgery plus postoperative adjuvant radiotherapy and concurrent chemoradiation for FIGO stage IIB cervical carcinoma: a retrospective study. Am J Clin Oncol 2010;33:583–6.
[11] Rotman M, Sedlis A, Piedmonte MR, Bundy B, Lentz SS, Muderspach LI, et al. A phase III randomized trial of postoperative pelvic irradiation in stage IB cervical carcinoma with poor prognostic features: follow-up of a gynecologic oncology group study. Int J Radiat Oncol Biol Phys 2006;65:169–76.
[12] Sedlis A, Bundy BN, Rotman MZ, Lentz SS, Muderspach LI, Zaino RJ. A randomized trial of pelvic radiation therapy versus no further therapy in selected patients with stage IB carcinoma of the cervix after radical hysterectomy and pelvic lymphadenectomy: a Gynecologic Oncology Group Study. Gynecol Oncol 1999;73:177–83.
[13] Mabuchi S, Morishige K, Isohashi F, Yoshioka Y, Takeda T, Yamamoto T, et al. Postoperative concurrent nedaplatin-based chemoradiotherapy improves survival in early-stage cervical cancer patients with adverse risk factors. Gynecol Oncol 2009;115:482–7.

[14] Mabuchi S, Okazawa M, Isohashi F, Ohta Y, Maruoka S, Yoshioka Y, et al. Postoperative whole pelvic radiotherapy plus concurrent chemotherapy versus extended-field irradiation for early-stage cervical cancer patients with multiple pelvic lymph node metastases. Gynecol Oncol 2011;120:94–100.
[15] Inoue T, Morita K. Long-term observation of patients treated by postoperative extended-field irradiation for nodal metastases from cervical carcinoma stages IB, IIA, and IIB. Gynecol Oncol 1995;58:4–10.
[16] Mabuchi S, Ugaki H, Isohashi F, Yoshioka Y, Temma K, Yada-Hashimoto N, et al. Concurrent weekly nedaplatin, external beam radiotherapy and high-dose-rate brachytherapy in patients with FIGO stage IIIb cervical cancer: a comparison with a cohort treated by radiotherapy alone. Gynecol Obstet Invest 2010;69:224–32.
[17] Mabuchi S, Isohashi F, Yoshioka Y, Temma K, Takeda T, Yamamoto T, et al. Prognostic factors for survival in patients with recurrent cervical cancer previously treated with radiotherapy. Int J Gynecol Cancer 2010;20:834–40.
[18] Halaska MJ, Novackova M, Mala I, Pluta M, Chmel R, Stankusova H, et al. A prospective study of postoperative lymphedema after surgery for cervical cancer. Int J Gynecol Cancer 2010;20:900–90.
[19] Kashima K, Yahata T, Fujita K, Tanaka K. Analysis of the complications after radical hysterectomy for stage IB, IIA and IIB uterine cervical cancer patients. J Obstet Gynaecol Res 2010;36:555–9.
[20] Huscher A, Bignardi M, Magri E, Vitali E, Pasinetti N, Costa L, et al. Determinants of small bowel toxicity in postoperative pelvic irradiation for gynaecological malignancies. Anticancer Res 2009;29:4821–6.
[21] Ohba Y, Todo Y, Kobayashi N, Kaneuchi M, Watari H, Takeda M, et al. Risk factors for lower-limb lymphedema after surgery for cervical cancer. Int J Clin Oncol 2011;16:238–43.
[22] Montz FJ, Holschneider CH, Solh S, Schuricht LC, Monk BJ. Small bowel obstruction following radical hysterectomy: risk factors, incidence, and operative findings. Gynecol Oncol 1994;53:114–20.
[23] Hasselle MD, Rose BS, Kochanski JD, Nath SK, Bafana R, Yashar CM, et al. Clinical Outcomes of Intensity-Modulated Pelvic Radiation Therapy for Carcinoma of the Cervix. Int J Radiat Oncol Biol Phys 2011;80:1436–45.
[24] Kamura T, Tsukamoto N, Tsuruchi N, Kaku T, Saito T, To N, et al. Histopathologic prognostic factors in stage IIb cervical carcinoma treated with radical hysterectomy and pelvic-node dissection — an analysis with mathematical statistics. Int J Gynecol Cancer 1993;3:219–25.
[25] Horn LC, Fischer U, Raptis G, Bilek K, Hentschel B. Tumor size is of prognostic value in surgically treated FIGO stage II cervical cancer. Gynecol Oncol 2007;107:310–5.
[26] Moore MJ, O'Sullivan B, Tannock IF. How expert physicians would wish to be treated if they had genitourinary cancer. J Clin Oncol 1988;6:1736–45.

Intraoperative Frozen Section Assessment of Myometrial Invasion and Histology of Endometrial Cancer Using the Revised FIGO Staging System

Hiromi Ugaki, MD, Toshihiro Kimura, MD, PhD,* Takashi Miyatake, MD, PhD,* Yutaka Ueda, MD, PhD,* Kiyoshi Yoshino, MD, PhD,* Shinya Matsuzaki, MD,* Masami Fujita, MD, PhD,* Tadashi Kimura, MD, PhD,* Eiichi Morii, MD, PhD,† and Takayuki Enomoto, MD, PhD**

Objectives: The objective of this study was to assess the value of intraoperative frozen section (IFS) diagnosis for myometrial invasion and histology of endometrial cancer using the revised International Federation of Gynecology and Obstetrics (FIGO) staging system.
Methods: The medical records of 303 patients with endometrial cancer who underwent surgery with intraoperative diagnosis at the Osaka University Hospital between January 1999 and December 2008 were reviewed. Intraoperative frozen section diagnosis was retrospectively analyzed for the accuracy rates of myometrial invasion and histology compared with the final diagnosis and with preoperative prediction by magnetic resonance imaging (MRI) and endometrial curettage.
Results: When using the previous FIGO staging system, the accuracy rate of IFS for the diagnosis of myometrial invasion was 77%, whereas the accuracy rate of preoperative prediction by MRI was 54%. However, using the newly revised FIGO staging system for myometrial invasion, the accuracy rate of IFS was 87% and the preoperative prediction by MRI was 82%. The accuracy rate of IFS for the diagnosis of histology was 71%, whereas the accuracy rate of preoperative prediction by endometrial curettage was 68%.
Conclusion: Although under the previous FIGO staging system IFS diagnosis was significantly more accurate than preoperative prediction by MRI, when using the newly revised FIGO staging system, there are no significant differences between the values of preoperative and intraoperative diagnoses. The accuracy of IFS, however, trends to be slightly better than the preoperative procedures of MRI and endometrial surface biopsy. Thus, IFS diagnosis is still useful for directing primary operative management.

Key Words: Endometrial cancer, Intraoperative frozen section, Revised FIGO staging system

Received October 19, 2010, and in revised form April 18, 2011.
Accepted for publication April 28, 2011.

(*Int J Gynecol Cancer* 2011;21: 1180–1184)

Endometrial carcinoma is a common gynecological cancer, and its incidence has been increasing during the last 3 decades. Early-stage endometrial adenocarcinoma of the uterine corpus is treated by surgical approaches such as total abdominal hysterectomy and bilateral salpingooophorectomy. This approach is the basic treatment of early-stage endometrial

Departments of *Obstetrics and Gynecology, and †Pathology, Osaka University Graduate School of Medicine, Suita, Osaka, Japan.
Address correspondence and reprint requests to Takayuki Enomoto, MD, PhD, Department of Obstetrics and Gynecology, Osaka University Graduate School of Medicine. 2-2, Yamadaoka Suita, Osaka 567-0871, Japan. E-mail: hirohiromimi@hotmail.com.

ISSN: 1048-891X
DOI: 10.1097/IGC.0b013e318221eb92
The authors declare that there are no conflicts of interest.
Supplemental digital content is available for this article. Direct URL citation appears in the printed text and is provided in the HTML and PDF versions of this article on the journal's Web site (www.ijgc.com).

cancer, but it is not considered adequate in all cases. According to the Study in the Treatment of Endometrial Cancer reported in 2009, there was no evidence of any benefit for systematic lymphadenectomy for endometrial cancer in overall, disease-specific, or recurrence-free survival.[1] However, the necessity for additional pelvic and para-aortic lymphadenectomy is still controversial because determining their involvement is still necessary for staging.

Creaseman et al[2] demonstrated that the incidence of lymph node metastasis increases with tumor grade, depth of myometrial invasion, cervical or adnexal involvement, lymphovascular invasion, and poor histological types. Patients with well-differentiated tumors or minimal to no myometrial invasion are considered to be at low risk, and a staging lymphadenectomy is often not performed. For patients with moderate to poorly differentiated tumors and myometrial invasion, the reported incidence of pelvic lymph node metastasis ranges from 5% to 34%; likewise, the incidence of para-aortic nodal involvement is 5% to 25%. For these reasons, lymphadenectomy is important for exact staging of the disease and for estimating the prognosis of intermediate high-risk disease, and has thus been evaluated in several studies. In addition, some authors have suggested that an extended nodal dissection results in better survival,[3,4] at least for intermediate-risk patients. And recently, Todo et al[5] found that para-aortic lymphadenectomy has survival benefits for patients at intermediate or high risk of recurrence, and that pelvic lymphadenectomy alone might be an insufficient surgical procedure for endometrial cancer in patients at risk of lymph node metastasis.

However, there are currently no major guidelines for surgical risk assessment in endometrial cancer.

In 1988, the International Federation of Gynecology and Obstetrics (FIGO) changed their method of staging of endometrial cancer from a clinical to a surgical approach, largely owing to the realization of the prognostic importance of intraoperative findings. Most studies that have ascertained the accuracy of intraoperative frozen section (IFS) analysis in stage I endometrial disease have found a good correlation with the final pathological diagnosis.[6–9] Based on these publications, IFS seems to be effective at identifying low-risk patients who can be spared from aggressive surgical staging, in contrast to the extreme surgical needs of intermediate high-risk patients. Intraoperative frozen section has been the standard procedure at our institution since the late 1990s for identifying low- or intermediate high-risk endometrial cancers.

TABLE 1. Accuracy rate of preoperative and frozen section diagnosis using previous FIGO staging system

	Curettage or D&C	MRI	Frozen Section
Histological type, %	68		71
Depth of myometrial invasion, %		54	77

D&C, dilatation and curettage.

TABLE 2. Comparison of MRI and paraffin section diagnosis for myometrial invasion of endometrial carcinoma in the revised FIGO staging system

		Permanent Section		
		<1/2	≧1/2	Total
MRI	<1/2	195	23	218
	≧1/2	30	55	85
	Total	225	78	303

The aim of our current retrospective analysis was to evaluate the accuracy of our IFS diagnosis to determine whether IFS is still a reliable tool for directing the surgical management of patients with endometrial cancer, compared to emerging preoperative evaluations. Since a newly revised staging was published by FIGO in 2009, we compared the effects of using the 2 different staging methodologies with that in previous reports.

MATERIALS AND METHODS

The medical records of women with endometrial cancer treated at the Department of Obstetrics and Gynecology of Osaka University Hospital between January in 1999 and December in 2008 were reviewed to determine the accuracy of their IFS diagnosis. All staged cases were included in this retrospective study. Patients with non–endometrial cancer of the uterus were excluded. During this 10-year period, 414 women with endometrial cancer were surgically treated. For 303 of these patients, an IFS was done; the medical records and histological diagnosis of these 303 cases were reviewed and included in our analysis. Intraoperative frozen section was not performed in cases where it was deemed likely to have an inconsequential influence on subsequent patient treatment, that is, in elderly and highly morbid patients, in cases of macroscopic lymph node metastasis, or in cases of endometrial cancer unexpectedly diagnosed only later at final pathology.

After gross examination, IFS was performed from the area that seemed to show the deepest myometrial invasion of the corpus. One or two slides were then microscopically examined by a single pathologist. Formalin-fixed, paraffin-embedded sections were made in parallel, which were decisive for postsurgical definitive diagnosis.

Accurate IFS was defined as having concordance between the frozen section report and the final report on the fixed section. The accuracy of the preoperative diagnosis was also compared with the final diagnosis. Preoperative diagnosis is determined histologically from dilatation and curettage or biopsy material. Myometrial invasion depth was analyzed by magnetic resonance imaging (MRI). We compared our preoperative tests, IFS, and permanent section results using both

TABLE 3. Comparison of frozen and paraffin section diagnosis for myometrial invasion of endometrial carcinoma in the revised FIGO staging system

		Permanent Section		
		<1/2	≧1/2	Total
Frozen section	<1/2	205	18	223
	≧1/2	8	60	68
	NTI	12	0	12
	Total	225	78	303

NTI, no tumor involvement.

the previous and recently revised FIGO staging systems. We used the χ^2 test for our statistical analysis.

RESULTS

Between 1999 and 2008, 414 women with uterine cancer had under surgical treatment at our Department. An IFS was performed in 303 of the cases; these were considered eligible for the present investigation. The details are shown in supplemental Tables 1–4 (http://links.lww.com/IGC/A46).

According to the final histopathological evaluation, most of the tumors, 92%, were classified as endometrioid adenocarcinoma. Histological subtypes associated with poor prognosis, serous adenocarcinoma and clear cell adenocarcinoma, were diagnosed in 4% and 2% of the patients, respectively. The other 2% was the total of mucinous adenocarcinoma and undifferentiated adenocarcinoma. Histopathological grading was grades 1, 2, and 3 in 43%, 32%, and 16% of the cases, respectively.

Table 1 shows the accuracy rate of preoperative and frozen section diagnosis for histological type and depth of myometrial invasion. The accuracy rate of histological types of preoperative diagnosis and of IFS was 68% (207/303) and 71% (215/303), respectively (P = 0.7998). There was no significant difference between the accuracy rate of diagnosis for histology on preoperative diagnosis and on frozen section diagnosis.

With regard to myometrial invasion, the accuracy rate of MRI was 54% (164/303). However, the accuracy rate of IFS was 77% (232/303). There was a significant difference between MRI and frozen section ($P < 0.0001$).

The underdiagnosis rates of preoperative MRI and IFS diagnosis were 34% (102/303) and 15% (46/303), respectively. On the other hand, the overdiagnosis rates of preoperative MRI diagnosis and IFS were 12% (37/303) and 4% (13/303), respectively. By frozen section, there were 12 cases in which no tumor involvement was detected.

TABLE 4. Total (histology and myometrial invasion) accuracy of previous versus revised FIGO staging

	Preoperative	Frozen Section
Previous staging accuracy, %	37	56
Revised staging accuracy, %	58	65

TABLE 5. Accuracy rate of MRI and frozen section diagnosis using the revised FIGO staging system

	MRI	Frozen Section
Depth of myometrial invasion (revised), %	82	87

Using the old FIGO staging system, the complete accuracy rate, which means an exact diagnosis of histology and depth of myometrial invasion was given, was 37% (117/303) for preoperative diagnosis and 56% (170/303) for IFS, respectively, which indicated that there was a significant difference between the accuracy of the 2 methods ($P < 0.0001$, Table 4).

Next, using the newly revised FIGO staging system, we evaluated how well myometrial invasion was detected by preoperative MRI versus IFS by comparing to permanent sections (Tables 2 and 3). The accuracy rate for preoperative MRI was 82%, and for IFS, it was slightly better, 87%, but this difference was not statistically significant (P = 0.8346) (Table 5). Likewise, the complete accuracy, namely, the histology concordant with depth of myometrial invasion, of preoperative diagnosis and frozen section, were 58% (176/303) and 65% (199/303), respectively (Table 5), with no significant difference between MRI and IFS (P = 0.3582). These accuracy rates improved 21% for preoperative diagnosis and 9% for IFS, respectively, from the old FIGO staging system.

Meanwhile, there were 113 cases of call discrepancy between the IFS diagnosis and the permanent slide diagnosis. The IFS and permanent diagnosis slides of these cases were reexamined by another pathologist under blinded conditions. We have deduced that the discrepancies were evenly split between 2 causes; they were based on tissue sampling errors in 56 of the cases and on pathologist error in the remaining 57 cases (supplemental Table 5, http://links.lww.com/IGC/A46).

DISCUSSION

There have been several reports regarding the accuracy of IFS diagnosis, such as those reports shown in Table 6. For the grade of endometrioid carcinoma in past reports, the accuracy rate ranged relatively widely: from 68% to 96%.

TABLE 6. Accuracy of IFS diagnosis

First Author	Year	N	Myometrial Invasion, %	Grade, %
Zorlu et al[10]	1993	59	90	92
Noumoff et al[8]	1991	60	72	68
Fanning et al[7]	1990	216	95	96
Malviya et al[11]	1989	55	97	95
This study		303	87	71